ASSESSMENT OF AN EFFECTIVE STRESS ANALYSIS FOR PREDICTING THE PERFORMANCE OF DRIVEN PILES IN CLAYS

Andrew J. Whittle

MITSG 93-01

Sea Grant College Program
Massachusetts Institute of Technology
Cambridge, Massachusetts 02139

Grant No: NA86AA-D-SG089

Project No: 89-DH-1

$4

Related MIT Sea Grant College Program Publications

Shaft Resistance of Piles in Clay. Azzouz, Amr S., Mohsen M. Baligh and Andrew J. Whittle. MITSG 90-7J. $1.

Undrained Cyclic Simple Shear Behavior of Clay with Application to Pile Foundations Supporting Tension Leg Platforms. Malek, Azziz M., Amr S. Azzouz, Mohsen M. Baligh and John T. Germaine. MITSG 87-20. $18.

Capacity of Offshore Friction Piles in Clay--Opportunity Brief #44.. MIT Marine Industry Collegium. MITSG 86-14 . $2.50.

Cone Penetration and Engineering Properties of the Soft Orinoco Clay. Azzouz, Amr S., Mohsen M. Baligh and Charles C. Ladd. MITSG 82-11. $5.

Please add $1 for shipping/handling and mail your check to :
MIT Sea Grant College Program, 292 Main Street, E38-300, Cambridge, MA 02139.

ASSESSMENT OF AN EFFECTIVE STRESS ANALYSIS FOR PREDICTING THE PERFORMANCE OF DRIVEN PILES IN CLAYS

A.J. WHITTLE
Department of Civil and Environmental Engineering,
Massachusetts Institute of Technology
77 Massachusetts Ave., Cambridge, MA02139, USA.

ABSTRACT:
Researchers have advocated systematic analyses, which model changes in effective stresses and soil properties through successive phases in the life of a pile, as a rational method for understanding the factors which control pile performance. Work at MIT has included the development of analytical models which simulate soil disturbance effects associated with pile installation (Strain Path Method), and constitutive models (e.g., MIT-E3) which describe the effective stress-strain behaviour of normally and lightly overconsolidated clays (OCR≤4) through successive phases in the life of the pile. This paper summarizes the role of these analyses in predictions of pile shaft behaviour. The results illustrate the effects of soil properties, mode of pile installation and other factors affecting the limiting skin friction which can be mobilized at the pile shaft. Predictive capabilities and limitations of the proposed 'objective analysis' are reviewed based on comparisons with high quality field data measured by the piezo-lateral stress (PLS) cell and by instrumented model pile tests.

1. Introduction

The geotechnical group at MIT has been involved in a sustained research effort to develop more reliable methods for predicting the capacity and performance of friction piles driven in clays. Originally, these efforts were motivated by the uncertainties involved in extrapolating empirical correlations from onshore pile load tests to offshore applications where much larger piles are used and where soil conditions often include deep layers of weak, normally and lightly overconsolidated clays. More recently, the work has focused on the performance of piles supporting Tension Leg Platforms (TLP; Whittle, 1987; Whittle et al., 1988; Malek et al., 1989).

The research makes the fundamental assumption that pile performance should be evaluated using a rational framework in which the changes in stresses and soil properties are described through successive phases in the life of a pile (Esrig et al., 1977; Randolph et al., 1979; Baligh & Kavvadas, 1980). For TLP piles this includes: a) the initial, in-situ conditions in the ground; b) pile installation; c) soil consolidation or 'set-up'; d) monotonic shearing due to quasi-static tensile forces imposed by mooring of the TLP superstructure; and e) cyclic shearing caused by storm waves. Due to the complexities of these pile-soil interactions, extensive research efforts have been required in four complementary lines of activity:

1. The formulation of analytical models which are capable of making realistic predictions of pile performance. This work has included the development of: a) the Strain Path Method (Baligh, 1985, 1986a,b) to describe the mechanics of the pile installation process; and b) effective stress soil models (MIT-E1, Kavvadas, 1982; and MIT-E3, Whittle, 1987) which can describe realistically the constitutive behaviour of K_0-consolidated clays which are normally to moderately overconsolidated (OCR≤4).
2. In-situ measurements on a closed-ended model pile shaft referred to as the Piezo-Lateral Stress Cell (PLS; Morrison, 1984; Azzouz & Lutz, 1986; Azzouz & Morrison, 1988). The PLS cell has the capability of providing simultaneous measurements of the total lateral stress, pore pressures and average skin friction acting on the shaft of a small diameter pile (D=3.83cm) during installation, consolidation and axial loading.
3. Extensive laboratory testing to support the analytical and field studies, and to develop more comprehensive understanding of complex aspects of clay behaviour. This work has included: a) test programs to characterize in-situ soil properties (e.g., Azzouz & Lutz, 1986); b) undrained cyclic direct simple shear testing to simulate pile-soil interaction during TLP storm loading conditions (e.g., Malek et al., 1989); and c)

measurement of anisotropic properties in the Directional Shear Cell (DSC) which are used to evaluate the constitutive models (e.g., Whittle et al., 1992).

4. Evaluation of pile shaft predictions was initially accomplished using PLS cell measurements (Whittle & Baligh, 1988; Azzouz et al., 1990). Subsequently, analytical predictions have been compared with field data from instrumented pile tests at a number of sites (e.g., Whittle, 1991b).

This paper describes typical predictions of pile shaft performance using Strain Path analyses in conjunction with the MIT-E3 soil model. The analyses provide objective predictions of soil stresses and pore pressures during installation, consolidation and axial loading, based on specified in-situ soil properties and stress conditions. The results illustrate the effects of stress history, mode of pile installation and other factors on the limiting skin friction which can be mobilized at the pile shaft. Predictive capabilities and limitations of the analyses are assessed from comparisons with high quality field data at a number of soft clay sites.

2. The Strain Path Method

Pile driving causes severe disturbances and leads to significant changes in the stresses, pore pressures and properties of the surrounding soils. The analysis of these installation effects represents a highly complex problem due to: a) high gradients of the field variables (displacements, stresses, strains and pore pressures) around the pile; b) large deformations and strains which develop in the soil; c) the complexity of the constitutive behaviour of soils, including non-linear, inelastic, anisotropic, and frictional response; and d) non-linear pile-soil interface characteristics. The Strain Path Method (SPM; Baligh, 1985) assumes that, due to the severe kinematic constraints in deep penetration, the deformations and strains in the surrounding soil are essentially independent of its shearing resistance and can be estimated with reasonable accuracy based only on kinematic considerations and boundary conditions. The application of the Strain Path Method for analyzing piles driven in low permeability clays assumes: a) there is no migration of pore water during penetration and hence, the soil is sheared in an undrained mode; b) pile driving can be modelled as a quasi-static (steady), deep penetration problem (i.e., there is no inherent difference due to pile installation by jacking or driving); and c) the deformations and strains can be estimated from the steady, irrotational flow of an incompressible, inviscid fluid around the pile (Baligh & Levadoux, 1980; Baligh, 1986a; Whittle et al., 1991). By considering two-dimensional deformations of soil elements, the Strain Path analyses provide a more realistic

framework for describing the mechanics of deep penetration than one-dimensional, cylindrical cavity expansion methods (CEM; e.g., Kraft, 1982; Randolph et al., 1979). On the other hand, the assumptions of strain controlled behaviour used in the Strain Path Method greatly simplify the penetration problem and avoid the complexity of large deformation finite element analyses (e.g., DeBorst & Vermeer, 1984; Kiousis et al., 1988).

Figure 1 compares SPM solutions of strain paths experienced by individual soil elements for two pile geometries: 1) a closed-ended (or fully plugged) pile of radius, R, with a rounded tip geometry (the 'simple pile'; Baligh, 1985); and 2) an open-ended pile of with aspect ratio, B/t=40 (where B=2R is the outside diameter, and t the wall thickness), which penetrates the soil in an unplugged mode (Chin, 1986). These solutions correspond to the two extreme modes of penetration for large diameter, open-ended pipe piles used in offshore foundations. The strain history at a point is fully described by three independent components of shear strain; E_1, E_2 and E_3 which correspond to triaxial, pressuremeter (cylindrical cavity expansion) and direct simple shear modes, respectively.

For the simple pile geometry, there is monotonic increase in the E_2 shear component as the pile tip passes the soil element while the components E_1 and E_3 exhibit reversals in direction (which are not included in CEM analyses). The overall magnitude of shear strain in the soil is described by the second invariant of deviatoric strains, $E= 1/\sqrt{2}\ \{E_1^2 + E_2^2 + E_3^2\}^{1/2}$ as shown in figure 2. At locations around the pile shaft (Fig. 2), there is an inner zone of soil which experiences much larger shear strain levels than can be imposed in conventional laboratory shear tests (E>10% at r/R<2) and is characterized also by large net changes in all three strain components (e.g., elements r_0/R=0.5, 0.2; Fig. 1a). At radial locations further from the pile shaft, E_1, E_3->0 (e.g., r_0/R=1.0; Fig. 1a) and the final strain state is controlled by the volume of soil displaced by the pile.

The unplugged, open-ended pile causes much less disturbance of the surrounding soil. The zone of high shear strains (E≥10%; Fig. 2b) is confined to a thin annulus (comparable to the thickness of the pile wall) around the shaft, while far field strain levels are controlled by the volume of soil displaced by the pile. In order to compare the strain levels for the open and closed-ended piles, it is convenient to normalize the radial dimensions by the equivalent radius of a solid section pile, $R_{eq}=\sqrt{Bt}$ (i.e., for B/t=40, R_{eq}=0.316R) as shown in figure 2b. The mode of penetration (closed vs. open-ended) also causes important differences in strain paths close to the pile wall, especially in the pressuremeter shear component, E_2.

In this presentation of the Strain Path Method, effective stresses, σ'_{ij}, are computed directly from the strain paths of individual soil elements using a generalized effective stress-strain soil model (see next section). This approach can be contrasted with previous total

stress analyses (Levadoux & Baligh, 1980; Baligh, 1986a; Teh & Houlsby, 1991) which compute shear stresses through a deviatoric stress-strain model, and introduce a separate constitutive relationship for shear induced pore pressures. The main advantage of the effective stress analysis is that the same soil model can be used to study stress changes during consolidation and pile loading.

The installation excess pore pressures around the pile shaft are computed from the effective stresses by satisfying conditions of radial equilibrium (Baligh, 1986b). Further predictions of excess pore pressure distributions around the tip of the pile are difficult to achieve due to approximations used in the Strain Path Method. The most reliable estimates of pore pressure distributions are obtained by solving equilibrium conditions in the form of a Poisson equation using finite element methods (Aubeny, 1992; Whittle & Aubeny, 1992)

3. The MIT-E3 Effective Stress Soil Model

The MIT-E3 model (Whittle, 1987, 1990, 1991a) is a generalized effective stress soil model for describing the rate independent behaviour of normally to moderately overconsolidated clays (OCR≤8) which exhibit normalized engineering properties. The model describes a number of important aspects of soil behaviour which have been observed in laboratory tests on K_0-consolidated clays but are not well described by most existing soil models:

1. There is no well defined linear region of soil behaviour, even at small strain levels or immediately following a reversal of loading.
2. The unload-reload behaviour of clays is characterized by a hysteretic response, but also involves small irrecoverable strains.
3. Clays exhibit anisotropic properties due to their consolidation history and subsequent straining.
4. In some modes of deformation, normally and lightly overconsolidated clays exhibit undrained brittleness.
5. Uniform, undrained cyclic loading of overconsolidated clays causes an accumulation of shear induced pore pressures. Thus coupling of volumetric and shear behaviour is essential to accurate modelling of overconsolidated clays under cyclic loading.

The model formulation comprises three components: 1) an elasto-plastic model for normally consolidated clays, which describes anisotropic properties and strain softening behaviour; 2) equations for the small strain non-linearity and hysteretic stress-strain response in unload-reload cycles; and 3) bounding surface plasticity for irrecoverable,

anisotropic and path dependent behaviour of overconsolidated clays. Other observations of clay behaviour, collectively referred to as 'rate effects' (e.g., variation in undrained shear strength with strain rate, undrained creep and secondary compression) are not described by the MIT-E3 model. The model uses 15 input parameters which are determined from standard types of laboratory tests:

1. One dimensional consolidation tests (either incremental oedometer or constant rate of strain consolidation) using a load sequence that includes at least one cycle of unloading-reloading and measurements of lateral effective stresses.
2 Undrained shear tests on K_0-consolidated clay including in triaxial compression (CK_0UC) at OCR=1, 2 and triaxial extension (CK_0UE) at OCR=1. These tests should be performed using SHANSEP consolidation procedures in order to ameliorate the effects of sample disturbance on the measured soil behaviour (Ladd & Foott, 1974).
3. Measurements of elastic shear wave velocity using either resonant column apparatus or field cross-hole tests. Alternatively, reliable measurements of the small strain stiffness can now be obtained from local strain measurements in triaxial tests (e.g., Jardine et al., 1984; Dyvik & Olson, 1989; Clayton et al., 1989; Goto et al., 1991).

The model input parameters have been selected for a number of clays using a standard procedure (Whittle, 1990). Extensive comparisons with measured data in undrained shear tests performed in different modes of shearing and with overconsolidation ratios (OCR) up to 8 have shown that the model a) gives excellent predictions of peak shear resistance and can describe accurately the non-linear stress-strain behaviour, but becomes less reliable for OCR≥4. The most comprehensive evaluations have been presented for Boston Blue Clay (BBC), a low plasticity (I_p=19-23%), illitic, marine clay of moderate sensitivity (s_t=3-7) whose engineering properties have been studied extensively at MIT (Whittle, 1990, Whittle et al., 1992). Figure 3 compares the computed and measured shear stress strain behaviour for K_0-normally consolidated BBC in the three modes of shearing which occur during pile installation (cf., Fig. 1):

The measured data in undrained triaxial compression and extension tests (CK_0UC and CK_0UE) at OCR=1 illustrate important aspects of the anisotropic behaviour of soft clays: The undrained shear strength in the compression mode (s_{uTC}/σ'_{vc}=0.33) is mobilized at very small shear strains (ε_{ap}≈ 0.3-0.5%) and there is a significant post-peak reduction in shear resistance. In comparison, the undrained shear strength in triaxial extension is mobilized at relatively large strain levels (s_{uTE}/σ'_{vc}≈0.14 at ε_{ap}>5%). There is a large difference in the undrained shear strengths in the two modes of shearing, s_{uTE}/s_{uTC}=0.42. The MIT-E3 model matches closely the measured undrained shear strengths in both modes of shearing, as well as the axial strain at peak resistance and post-peak strain softening. The

measurements in monotonic compression and extension tests are part of the data set used to select input parameters and hence, these comparisons do not constitute an evaluation of model predictions. Model predictions for an undrained triaxial test with a single unload-reload cycle (i.e., two reversals of strain direction) are also shown in figure 3a. The model describes closely the non-linear and hysteretic nature of the unload-reload process, but tends to overpredict the stiffness during reloading.

Figure 3b compares predictions with measurements in undrained Direct Simple Shear tests (CK_0UDSS) using a Geonor simple shear apparatus. This mode of shearing is also directly relevant to predictions of pile-soil behaviour in axial loading (e.g., Randolph & Wroth, 1981; Azzouz et al., 1990) and is discussed in more detail in section 6. The MIT-E3 model gives very good predictions of the shear stress strain response in tests with monotonic shearing and with reversals of strain direction. The model is in excellent agreement with the measured peak shear resistance ($\tau_{max}/\sigma'_{vc}=0.21$) but tends to overestimate the stiffness in reloading.

The pressuremeter shear mode (E_2; Fig. 1) is especially important for estimating the effects of pile installation and can be simulated in laboratory element tests using more sophisticated equipment such as the True Triaxial Apparatus (TTA) or Directional Shear Cell (DSC). Unfortunately, there is very little data of this type reported in the literature. Figure 3c compares model predictions with data reported by Wood (1981) using the Cambridge University TTA. The model predictions match the measured peak shear resistance, $s_{uPM}/\sigma'_{v0}=0.21$, which is mobilized at a shear strain, $\gamma \approx 5\%$. Further comparisons with more comprehensive pressuremeter tests in the DSC at OCR=4 (O'Neill, 1985; Fig. 3c) show similar predictive accuracy for the peak shear resistance, but confirm that the model tends to overestimate the pre-peak shear stiffness.

The shear resistance at large strain levels is important in predicting stress conditions close to the pile shaft during installation. However, it is difficult to obtain reliable large strain measurements in laboratory tests due to non-uniformities in stress conditions, strain localization etc. The predictions in figure 3 show that there is a large post-peak reduction in the shear resistance of K_0-normally consolidated BBC in undrained triaxial compression ($s_{ur}/s_u=0.4$), but negligible softening in the pressuremeter shear mode. Strain softening measured in Direct Simple Shear tests may be partly attributed to non-uniform stress conditions in the Geonor apparatus (e.g., DeGroot et al., 1992).

Although it is not possible to duplicate the complex strain paths caused by pile installation using existing laboratory tests, the results in figure 3 demonstrate the predictive capabilities of MIT-E3 and provide a sound basis for applying the model in conjunction with SPM analyses.

4. Pile Installation

4.1 Predictions of Installation Conditions

Figure 4 presents Strain Path (SPM) and Cavity Expansion (CEM) predictions of installation stresses and pore pressures around the shaft of a pile in K_0-normally consolidated BBC using the MIT-E3 soil model. The individual stress components are normalized by the in-situ vertical effective stress, σ'_{v0}, while radial dimensions are related to the equivalent radius of a solid section pile, R_{eq}, in order to unify results for the two limiting modes of pile penetration (plugged and unplugged). The two principal parameters of interest in these analyses are the excess pore pressures, $\Delta u_i/\sigma'_{v0}$, and radial effective stresses, $K_i=\sigma'_r/\sigma'_{v0}$ which can be measured at the pile shaft. The results in figure 4 show the following:

1. For a normally or lightly overconsolidated clay, undrained shearing generates positive shear induced pore pressures and a corresponding net reduction in the mean effective stress, σ'/σ'_{v0}, close to the pile shaft. Differences in the magnitude of σ'/σ'_{v0} for SPM and CEM analyses ($r/R_{eq}\leq 6$; Fig. 4a) reflect how the anisotropic and strain softening properties described by the MIT-E3 model are affected by differences in strain histories.
2. The effects of the analysis used to model installation can be seen most clearly in predictions of the radial effective stress, σ'_r/σ'_{v0}, and cavity shear stress, q_h/σ'_{v0} (where $q_h=[\sigma'_r-\sigma'_\theta]/2$ is the maximum shear stress in the horizontal plane) The strain path method predicts very low radial effective stresses (K_i=0.08-0.10) and cavity shear stresses (q_h/σ'_{v0}->0) acting at the pile shaft for both modes of penetration. This means that the radial effective stress is similar in magnitude to the mean effective stress (i.e., $\sigma'_r/\sigma'_{v0}\approx\sigma'/\sigma'_{v0}$) for $r/R_{eq}\leq 15$. In contrast, CEM analyses give higher values of radial effective stress σ'_r/σ'_{v0} and predict that $\sigma'_r/\sigma'_{v0}>\sigma'/\sigma'_{v0}$ over a wide radial zone ($r/R\leq 20$). The cavity shear stress, q_h/σ'_{v0}=0.20, is approximately constant for $r/R<7$ and can be deduced from the pressuremeter shear behaviour described in figure 3c. Strain path predictions of σ'_r/σ'_{v0} are affected significantly by soil properties (including strain softening), while Baligh and Levadoux (1980) show that the geometry of the pile tip has an important effect on the cavity shear stress close to the shaft.
3. The excess pore pressures at the pile shaft are obtained from conditions of radial equilibrium and hence depend on the entire field of effective stresses in the soil. The results in figure 4a show that undrained pile installation generates large excess pore

pressures in the soil which extend to a radial distance r/R=20-30. Although both CEM and SPM predict a similar accumulation of excess pore pressure in the far field ($3 \leq r/R \leq 30$), there are significant differences in the distribution close to the pile shaft ($r/R \leq 3$). The net result is that the cavity expansion method predicts excess pore pressures which are typically 20-25% larger than those obtained from corresponding strain path analyses. The characteristic shapes of the pore pressures distributions (CEM and SPM; Fig. 4a) have been discussed in detail by Baligh (1986b) and are not affected significantly by the modelling of soil behaviour.

4. The mode of penetration (Figs. 4a, 4b) only affects the magnitude and distribution of stresses and pore pressures close to the pile wall, $r/R_{eq} \leq 3$. The strain path predictions of cavity shear stress, radial and mean effective stress components acting at the shaft are very similar for both modes of penetration, while the excess pore pressures are slightly smaller for the unplugged pile. It is interesting to note that the strain path method actually predicts slightly larger shaft pore pressures than the CEM analyses for the unplugged pile.

4.2 Evaluation of Installation Predictions

Simultaneous measurements of shaft pore pressures and lateral earth pressures (radial total stresses) during installation have been obtained at a number of sites using a) instrumented pile shaft elements or probes (PLS cell, Morrison, 1984; t-z and x-probes; Bogard et al., 1985; IMP, Coop & Wroth, 1989), and b) instrumented model piles (Karlsrud & Haugen, 1985; Karlsrud et al., 1992; Bond et al., 1991). Further measurements of installation pore pressures are associated with the development of in-situ testing devices such as the piezocone and include both field tests and laboratory experiments in large scale calibration chambers. The reliability of these measurements depends, in large part, on the design of the instrumentation (response time, calibration for thermal changes, etc.) and quality of test procedures (de-airing of porous filters etc.). The method of installation (driving versus jacking, rate of penetration, delay times, etc.) can also affect the measured parameters (e.g., Azzouz & Morrison, 1988) due to factors such as partial drainage which are not considered in the analysis.

Figure 5 compares the predictions of excess pore pressures at the pile shaft with measurements obtained during steady penetration in BBC using the PLS cell (Morrison, 1984; Azzouz & Morrison, 1988) as functions of the stress history (OCR). The measured data are very consistent at low OCR, but exhibit large scatter in the more overconsolidated clay due to the presence of sand seams etc. In general, the strain path predictions underestimate the measured excess pore pressures, particularly at low OCR, while there is

better agreement with results from CEM analyses. The figure also includes field measurements from pile and penetrometer tests compiled from five other sites. The results tend to confirm the previous assessment of Baligh and Levadoux (1980) that there is no well defined correlation between the shaft pore pressures and clay type (as described by plasticity index, I_p), stress history (OCR; Fig. 5), undrained shear strength or sensitivity (s_t). At low OCR, the excess pore pressures measured at five sites are in the range $\Delta u_i/\sigma'_{v0}$=2.0±0.4. Significantly lower installation pore pressures ($\Delta u_i/\sigma'_{v0}$=1.2-1.3; Fig. 5) have been reported recently from large-scale, laboratory calibration chamber tests in kaolin (May, 1987; Nyirenda, 1989).

In principle, measurements of the radial distribution of excess pore pressures (using piezometers in the surrounding soil) can provide a more comprehensive evaluation of the strain path predictions. In practice, these measurements are difficult to obtain (especially in the critical region close to the shaft, 1≤r/R≤5) due to a) interference of the measuring device and the soil deformations, and b) uncertainties in the alignment and position of the piezometers. Figure 6 compares MIT-E3 predictions of the excess pore pressure distribution for BBC at OCR=1.0, 2.0 and 4.0 with 1) field measurements (Roy et al., 1981) around an instrumented pile (R=11cm) installed in highly sensitive, structured St Alban clay (liquidity index, I_L≥2) at OCR=2.3, and 2) measurements around the shaft of a cone penetrometer installed in K_0-normally consolidated kaolin (R=1.26cm) within a large calibration chamber (of radius, R_c=50cm). The SPM predictions at OCR=1 are in very good agreement with penetration pore pressures measured in kaolin. The predictions at OCR=2 underestimate both the magnitude and the radial extent of the zone of pore pressure accumulation in the St Alban clay. These results indicate that the main source of discrepancy between strain path predictions and measured pore pressures are the effective stresses in the far field (r/R≥5-6, where E≤1%, Fig. 2a), which are affected by small strain properties of the clay and can be addressed through further refinement of the constitutive model. In contrast, CEM analyses do not describe accurately the shape of the pressure distribution and hence, overestimate $\Delta u_i/\sigma'_{v0}$ at the shaft while underestimating pore pressures measured in the far field.

Overall, it is not possible to draw definitive conclusions from the results presented in figures 5 and 6. Installation pore pressures around the pile shaft are very difficult to evaluate due to the complexity of the analysis and the sensitivity of the predictions to soil non-linearity and inelastic behaviour. Predictions using the MIT-E3 model (with input parameters for BBC) suggest that, although the strain path method underestimates the installation excess pore pressures, it provides a more consistent description of the lateral distribution of effective stresses than corresponding CEM analyses.

Radial effective stresses, K_i, during pile installation are obtained by subtracting the installation pore pressures from measurements of total radial stress at the same location. Figure 5 shows that pile installation in normally and lightly overconsolidated clays generates large excess pore pressures in the surrounding soil. It is therefore apparent that small errors in the measured pore pressures (and/or total stress) can affect significantly the computed radial effective stress. Azzouz and Morrison (1988) report K_i=0.05-0.20 from PLS measurements in the lower Boston Blue Clay (OCR=1.2±0.1) which are in excellent agreement with strain path predictions (cf., Fig. 4). Very small values of K_i are also reported from instrumented pile tests in other sensitive, low plasticity clays (Haga; Karlsrud & Haugen, 1985; Onsøy, Karlsrud et al., 1992). Significantly larger radial effective stresses, K_i=0.38-0.54, were measured in the more plastic, less sensitive Empire clay (Azzouz & Lutz, 1986) and are also in good agreement with strain path predictions using the MIT-E3 model (K_i=0.37-0.45; Whittle & Baligh, 1988).

5. Consolidation

5.1 Non-linear Analysis of Radial Consolidation

After pile installation, soil consolidation occurs due to the dissipation of excess pore pressures around the pile. For shaft locations far from the pile tip and the mudline, it is assumed that excess pore pressures dissipate radially away from the shaft and there are concomitant changes in the effective stresses due to radial displacements of the soil. Thus the underlying mechanism of pile 'set-up' (changes in shaft capacity with time after installation) is attributed to changes in effective stresses in the soil at (or close to) the pile-soil interface due to radial consolidation.

Previous studies (Randolph et al., 1979; Baligh & Levadoux, 1980; Baligh & Kavvadas, 1980) have shown that predictions of the change in radial effective stress acting on the pile shaft during consolidation are strongly affected by non-linearity of the soil. For the special case of a linear, isotropic (and elastic) soil, the decrease in excess pore pressure is exactly balanced by an increase in radial effective stress, such that at the end of consolidation, $\sigma'_{rc}=\sigma'_{ri}+\Delta u_i$. Comparison with measured data shows that this leads to a vast overprediction of the set-up around the pile shaft in soft clay deposits. Thus, comprehensive analyses of the coupled non-linear consolidation (i.e., coupling of total stresses and pore pressures; non-linear effective stress-strain and permeability properties of the soil) are required in order to achieve reliable predictions of the set-up process. The

analyses described in this section solve the radial consolidation by non-linear finite element methods using with the following assumptions:

1. Initial conditions are described by the radial distributions of effective stresses and pore pressures predicted around the shaft during pile installation using the Strain Path Method.
2. The non-linear effective stress-strain response of soil elements around the pile shaft is represented consistently by the MIT-E3 model (i.e., with the same input parameters used during pile installation) The compressibility of the soil is a function of the radial location of the soil element (due to installation disturbances) and varies with effective stresses during consolidation.
3. Non-linearities associated with changes in soil permeability are not considered in the analysis. This assumption implies that the radial permeability is spatially constant after pile installation and that changes in permeability during consolidation can be neglected. Recent experimental data from model tests on resedimented BBC suggest that permeability can decrease by up to a factor of 3 at locations close to the pile shaft following complete set-up (Ting et al., 1990). However, these changes in permeability are small compared with inherent uncertainties in the measurement of permeability of natural soil deposits and with non-linearities associated with soil stiffness predicted during consolidation.

Figure 7 summarizes predictions of the excess pore pressures, $\Delta u/\sigma'_{v0}$, radial total and effective stresses ($H=(\sigma_r-u_0)/\sigma'_{v0}$, and σ'_r/σ'_{v0}, respectively) acting at the shaft of a pile installed in K_0-normally consolidated BBC. The results are presented using a dimensionless time factor, T, which is defined as:

$$T = \frac{\sigma'_0 \, k \, t}{\gamma_w \, R_{eq}^2} \qquad (1)$$

where $\sigma'_0=1/3(1+2K_0)\sigma'_{v0}$ is the in-situ mean effective stress in the ground, t is the time, R_{eq} is the equivalent radius, k is the (horizontal) coefficient of permeability, and γ_w is the unit weight of water.

The principal parameter of interest in the analysis is the magnitude of the radial effective stress acting on the pile shaft after full dissipation of excess pore pressures $K_c=\sigma'_{rc}/\sigma'_{v0}$. For the closed-ended pile example shown in figure 7, the analyses using the Strain Path Method and MIT-E3 model predict a final set-up stress ratio, $K_c=0.37$ (Fig. 7a) which is significantly smaller than the initial, in-situ earth pressure coefficient ($K_0=0.48$), while comparable linear, consolidation analyses (i.e., based on the same installation conditions) would give $K_c=1.28$ ($=K_i+\Delta u_i/\sigma'_{v0}$). Thus, the predictions of set-up stresses vary by a factor of 3 to 4 depending on the modelling of non-linear soil behaviour. The set-

up stresses predicted for the open-ended (unplugged) pile are approximately 25% lower than for the closed-ended pile.

Predictions using cavity expansion analysis of pile installation (CEM) show significantly higher set-up stresses (K_c=0.72; Fig. 7a). This result is primarily due to the predicted initial conditions (K_i=0.45, Fig. 4) since the net change in radial effective stress during consolidation is relatively small.

Further insights into factors affecting the set-up predictions can be achieved by introducing the dimensionless stress ratios show in figure 7b: The excess pore pressure ratio (degree of consolidation), $U=\Delta u/\Delta u_i$, depends primarily on the normalized radial distribution of installation excess pore pressures ($\Delta u/\Delta u_{sh}$, where Δu_{sh} is the excess pore pressure at the pile shaft; Baligh & Levadoux, 1980). Strain path analyses for both closed and open-ended piles give very similar rates of consolidation (U vs T; Fig. 7b), while CEM predictions show more rapid dissipation of pore pressures for $U \geq 0.3$. The set-up effective stress ratio, K/K_c, illustrates most clearly the importance of the installation analysis (SPM vs CEM). The strain path results in figure 7b show that the largest change in set-up stresses occurs over the time period $0.01 \leq T \leq 1.0$. In contrast, the total stress release ratio, H/H_i, is primarily a function of the soil behaviour. Factors affecting H/H_i include the shear behaviour at large shear strains (i.e., during installation) and the radial compressibility during consolidation. The MIT-E3 predictions for normally consolidated BBC show H_c/H_i =0.25-0.3 (Fig. 7b), while results obtained for other soils and stress histories range from H_c/H_i=0.2 to 0.6 (Whittle & Baligh, 1988).

5.2 Evaluation of Shaft Stresses during Set-Up

Effective stresses at the pile shaft are currently calculated from measurements of total stresses and pore pressures during consolidation (e.g. Azzouz & Morrison, 1988; Karlsrud & Haugen, 1985), although direct measurements of σ'_r have been reported recently in a highly overconsolidated clay (using effective pressure transducers; Karlsrud et al., 1992). In addition to obvious sources of experimental errors, there are two main difficulties in determining accurately the set-up stress ratio, $K_c=\sigma'_{rc}/\sigma'_{v0}$ (Azzouz et al., 1990) 1) incomplete consolidation, and 2) limitations of total lateral stress measurements.

The time delay required to achieve complete consolidation depends on the (equivalent) radius of the pile and the soil properties (permeability and compressibility). For example, Azzouz and Morrison (1988) report consolidation times of 4-8 days using the PLS cell (R≈1.9cm), while 1-2 months of set-up are typical of instrumented model piles with R=7-10cm (e.g., Karlsrud et al., 1992). In practice, K_c values are frequently quoted from measurements obtained with incomplete consolidation. In these situations, calculations

using measurements of σ_r and u tend to underestimate K_c; while those based on σ_r and u_0 (in-situ pore pressures) overestimate the effective set-up stress.

Measurements of pore pressures at later stages of consolidation can easily be checked through comparisons with known values of u_0. Thus, most of the uncertainties in σ'_{rc} are due to possible errors in total stress measurements which are commonly caused by: a) significant seating errors (zero reading) of the σ_r cell due to soil arching; b) the cross sensitivity of σ_r measurements to changes of the axial load in the pile; and c) the changes of total stress cell calibration with time after installation (zero shift). Significant improvements in the design of instrumentation (e.g. Bond et al., 1991; Karlsrud et al., 1992) represent an important contribution in reducing these errors.

Figure 8 compares the predictions of the effective stresses at full set-up with measurements obtained by the PLS cell in BBC (Morrison, 1984; Azzouz & Morrison, 1988) as functions of the stress history. The predicted K_c increases significantly with the OCR and range from K_c=0.37-0.42 at OCR=1 (for K_{0NC}=0.48-0.53) to K_c=1.1-1.30 at OCR=4 (where K_0=0.75-1.0). Although the set-up stress is similar in magnitude to the in-situ earth pressure, the average ratio K_c/K_0 ranges from 0.8 at OCR=1, to 1.4 at OCR=4. The PLS measurements are generally in very good agreement with the predictions and support the result that K_c increases with OCR, although there is a large scatter in the data for OCR≥3. The figure also includes field measurements of K_c at three other sites (Empire, Onsøy and Haga) together with laboratory tests on a miniature pile in kaolin. There is consistent agreement in the data obtained for three clays of moderate sensitivity (s_t=3-7; BBC, Onsøy and Haga); while higher set-up stresses are measured in the Empire clay and kaolin. Although the predictions of K_c for Empire clay (Fig.8) are 50-60% higher than those described for BBC, they still underpredict the PLS measurement in zone I (cf., Azzouz & Lutz, 1986). No analyses (using SPM and MIT-E3) have yet been performed for the kaolin, however, Azzouz et al. (1990) suggest that these data are affected significantly by boundary conditions.

The results in figure 8 indicate that the combination of strain path installation analyses and non-linear radial consolidation with MIT-E3 are capable of providing good predictions of the effective stresses at the end of set-up. However, more comprehensive predictions are necessary to establish how predictions of K_c are related to engineering properties of the soil.

Figures 9 and 10 present a detailed evaluation of the predictions of set-up behaviour at the pile shaft based on PLS measurements (Morrison, 1984) in the lower deposit of BBC (OCR=1.3±0.1). The consolidation predictions are presented at OCR=1.0 and 1.5 using a modified time factor, $T = \sigma'_p kt / \gamma_w R^2$, where σ'_p is the vertical preconsolidation stress.

This time factor unifies predictions of the consolidation rate (U vs T; Fig. 9b) for normally and lightly overconsolidated BBC (Aubeny, 1992). Measurements of the total radial stress and excess pore pressure ratios (H/H_i and U, respectively) are then compared with the predictions (Fig. 9). An average coefficient of horizontal permeability, $k_h=8\times10^{-7}$cm/sec is selected from laboratory CRS and constant head measurements which range from $3.0\times10^{-8} \leq k_h \leq 1.5\times10^{-7}$cm/sec in the lower BBC (no significant variation with depth in the deposit). The predictions are in excellent agreement with the measured excess pore pressure ratio throughout consolidation, but tend to underestimate slightly the reduction in total radial stress. Effective stress changes at the pile shaft during consolidation, K(T), are calculated from the average measurements of total radial stress and excess pore pressure (Fig. 10). These data agree with predictions of radial effective stresses for OCR=1.5 and confirm the capabilities of the analysis for describing pile shaft performance throughout the set-up process.

5.3 Stress Conditions in the Soil after Consolidation

Predictions of the stress state in the soil after consolidation have an important influence on the subsequent prediction and interpretation of pile shaft capacity. Figure 11 presents predictions of the stress distribution around the pile shaft in BBC at OCR=1 and 2. The results show a net reduction in the mean effective stress (σ'_c/σ'_{v0}) in the soil around the pile (i.e., compared to the in-situ conditions). Radial consolidation produces cavity shear stresses (q_{hc}/σ'_{v0}) in the soil extending to a distance $r/R\leq3$ (cf. Fig. 4). At the pile shaft, σ'_{rc} is the major principal effective stress, while $\sigma'_{\theta c}/\sigma'_{rc}=K_{0NC}$. Figure 12 compares the volumetric behaviour (i.e., mean effective stress and volumetric strain) of soil elements adjacent to the pile shaft with the K_0-Virgin Consolidation Line (K_0-VCL) predicted for the undisturbed clay (using MIT-E3). Pile installation (paths A-B) generates large shear induced pore pressures (reductions in σ') associated with severe shearing of the soil at constant water content. During set-up (paths B-C) the soil elements do not return towards the K_0-VCL, but instead exhibit a more compressible behaviour such that the final states of stress (C_1, C_2) coalesce on a new re-consolidation line which lies parallel to the compression of the undisturbed clay. This result is qualitatively similar to the observations of the consolidation behaviour of remoulded Haga clay reported by Karlsrud and Haugen (1985).

6. Axial Pile Loading

6.1 Analysis of Shaft Capacity

This section focuses on predictions of the limiting skin friction, f_s, which is mobilized at the pile shaft after full dissipation of the installation excess pore pressures. The analyses are restricted to the case of a long, rigid pile for which the pile tip and the mudline have negligible effects on the shaft resistance. Even after introducing this simplification, there are three main factors which complicate significantly the prediction and interpretation of pile-soil interaction during axial loading:

1. Although slip surfaces are constrained to form parallel to the pile shaft, the actual slippage may occur either at the pile-soil interface or within the surrounding soil mass. Slippage at the interface is of practical importance when the limiting angle of interface friction, δ', is less than the effective stress obliquity, α'_p, mobilized along vertical planes in the soil at peak shear resistance (i.e., $\alpha'_p=\tau_f/\sigma'_{rf}$).
2. The shear resistance of the soil is controlled by effective stresses and properties around the shaft prior to loading. The previous sections have shown that relatively sophisticated analyses can predict many aspects of the set-up behaviour measured at the shaft for piles installed in normally and lightly overconsolidated clays. However, many aspects of the predictions cannot be evaluated from field measurements and hence, represent a source of uncertainty in the subsequent comparison with measured capacity.
3. Drainage conditions during pile loading are not well defined. For most conventional test procedures, the pile is loaded to failure over a period of several hours, such that the surrounding soil is sheared under conditions of partial (or complete) drainage which must be interpreted using effective stress methods.

For piles installed in lightly overconsolidated clays, the critical conditions (i.e., minimum shaft capacity) are likely to occur when the pile is loaded rapidly with no radial migration of pore water, and hence undrained shearing of the clay. In this situation, the mode of deformation corresponds to the shearing of concentric cylinders around the pile shaft (i.e., γ_{rz} is the only non-zero strain component), while vertical equilibrium controls the radial distribution of shear stresses ($\tau_0 R = \tau r$, where τ_0 is the interface shear stress). Figure 13a shows MIT-E3 predictions of the normalized effective (σ'_r/σ'_{rc}, τ/σ'_{rc}) and total stress paths ($[\sigma_r - u_0]/\sigma'_{rc}$, τ/σ'_{rc}) acting in the vertical plane for undrained shearing of soil elements adjacent to the pile shaft in Boston Blue Clay. The results show the following:

1. The initial stress history of the soil does not affect the normalized effective stress paths predicted at the pile shaft after full re-equilibration of the installation excess pore pressures for OCR≤4.

2. The peak shear resistance of the soil elements can be described by an undrained strength ratio, $\rho = \tau_f/\sigma'_{rc} \approx 0.26$ (Whittle et al., 1988; Azzouz et al., 1990) which is mobilized at an effective stress obliquity, $\alpha'_p \approx 24^0$ (which is significantly lower than the reference critical state friction angle measured in triaxial compression tests, $\phi'_{TC}=33.4^0$).
3. There is a reduction in the radial effective stress, $\Delta\sigma'_{rf}/\sigma'_{rc} \approx 0.4$, together with positive excess pore pressures, $\Delta u_f/\sigma'_{rc} \approx 0.4\text{-}0.5$, and a small net increase in the total stress ($[\sigma_r - u_0]_f/\sigma'_{rc} \approx 1.05$, Fig. 13a) for shearing up to peak shaft resistance. The zone of excess pore pressures extends laterally to a distance, $r/R \leq 5$ (Fig. 13b).

The analyses can be extended to consider the radial distribution of undrained shear resistance $\rho(r/R)$ by computing the response of individual soil elements to the same mode of shearing. The predictions in figure 11 show that a) the shaft capacity is limited by the undrained shear strength of soil elements adjacent to the pile, and b) the shear resistance, $\rho(r/R)$, is proportional to the mean effective stress predicted at the end of consolidation (σ'_c/σ'_{rc}) for $r/R \leq 2$.

The mode of shearing assumed for soil elements adjacent to the pile shaft is identical to that imposed in laboratory constant volume (undrained) Direct Simple Shear (DSS) tests. Thus, it is useful to compare model predictions of soil behaviour for the remoulded soil around the pile shaft with that of the undisturbed K_0-consolidated clay in undrained Direct Simple Shear tests. Figure 13a shows MIT-E3 predictions of the normalized effective stress paths (σ'_v/σ'_{vc}, τ/σ'_{vc}) for K_0-consolidated BBC at OCR=1.0, 1.2 and 1.5. The undrained strength ratio ($s_{uDSS}/\sigma'_{vc}=0.25$) and effective stress path of the undisturbed clay at OCR =1.2 are in close agreement with the normalized behaviour predicted at the pile shaft, although there is a difference ($\psi=20^0$ versus $\alpha'_p=24^0$) in the stress obliquity mobilized at peak shear resistance. Differences in the normalized response at the pile shaft and the K_0-normally consolidated clay (OCR=1.0) can be attributed mainly to the predicted ratios of effective stress components in the soil at the end of consolidation (i.e., $\sigma'_{rc}:\sigma'_{zc}:\sigma'_{\theta c}$ versus $\sigma'_h=K_{0NC}\sigma'_v$) (Whittle, 1987).

Azzouz et al. (1990) have proposed that the undrained strength ratio, ρ, can be used to provide realistic estimates of the limiting value of f_s for the design of friction piles in lightly overconsolidated clays (OCR≤4). The limiting skin friction is written as:

$$f_s = K_c \rho \sigma'_{v0} \qquad (2)$$

where σ'_{v0} is the in-situ effective overburden stress.

This method re-expresses the well known β parameter ($\beta=f_s/\sigma'_{v0}$; Chandler, 1968; Burland, 1973) as the product of the lateral earth pressure coefficient, K_c, and the undrained shear strength ratio, ρ, of the soil adjacent to the pile shaft. Predictions for normally and lightly overconsolidated clays show that K_c is affected by the stress history of

the clay (OCR) and by its sensitivity, while ρ can be estimated from the strength ratio measured in undrained direct simple shear tests on the undisturbed clay at OCR≈1.2.

In principle, lower values of the limiting skin friction can occur if the interface friction angle, δ', is smaller than the effective stress obliquity, α'_p, mobilized at peak shear resistance in the soil. Measurements in the ring shear apparatus show that δ' depends on numerous factors including soil mineralogy and fabric, consolidation and shear history, rate of shearing, interface roughness and hardness (Lemos, 1986). Comparisons between MIT-E3 predictions of α'_p for a number of clays (in the range, $\alpha'_p=17^0$-24^0) and recent correlations for δ' (Jardine & Christoulas, 1991) show that $[\alpha'_p-\delta'] \leq 5^0$, and suggest that interface slippage can reduce the calculated undrained shear resistance, ρ, by up to 25%.

The model predictions also provide a basis for evaluating drainage conditions during pile loading. Figure 13b shows the radial distribution of stresses and excess pore pressures at conditions corresponding to peak undrained shear resistance in the soil at the pile shaft (for BBC at OCR=1). Subsequent dissipation of the excess pore pressures provides some guidance on the characteristic time required to achieve undrained loading of the pile. Figure 13c compares predictions of the uncoupled dissipation of excess pore pressures generated during installation and axial loading. For the PLS cell (R=1.92cm) installed in the lower deposit of BBC (c_h≈0.02cm^2/sec; Baligh & Levadoux, 1980), the predictions show t_{50}≈40secs, while undrained conditions are only achieved when the shaft is loaded to failure within 1sec. In this situation, the soil around the pile is sheared at an average strain rate which is significantly higher than that imposed in conventional laboratory CK_0UDSS tests ($\dot{\gamma}$=5%/hr). Data from CK_0UDSS tests with t_f≈1-10secs (e.g., Lacasse, 1979) show a 15-25% increase in the undrained strength ratio and develop much smaller shear induced pore pressures compared to tests performed at conventional strain rates. These measurements suggest that predictions using the rate independent MIT-E3 model (Fig. 13a) will tend to underestimate the shaft resistance and overestimate the excess pore pressures for undrained loading.

The one-dimensional (radial) predictions described in this section implicitly assume that the pile shaft performance is similar for loading in either axial compression or tension. In practice, the local shaft resistance can be affected by factors such as proximity to the pile tip (e.g., Lehane & Jardine, 1992) or residual axial loads in the pile (e.g., Whittle, 1991b). More comprehensive two-dimensional analyses of set-up and loading are required in order to evaluate these effects. However, some insight can be obtained from simple model predictions of material behaviour in laboratory element tests. For example, residual axial loads in the pile generate shear stresses during set-up at the pile-soil interface (i.e., $\rho_c=\tau_c/\sigma'_{rc}$). These effects can be simulated in laboratory CK_0UDSS tests by consolidating

the soil under an applied shear stress, τ_c/σ'_{vc}. Figure 14 compares MIT-E3 predictions with the measured effective stress paths and shear stress-strain response for CK_0UDSS tests on normally consolidated BBC for consolidation shear stress ratios $-0.2 \leq \tau_c/\sigma'_{vc} \leq 0.2$. The results show the following:

1. Specimens consolidated with shear stresses applied in the same direction as the subsequent undrained loading ($\tau_c/\sigma'_{vc}>0$) exhibit higher undrained shear strengths, smaller shear induced pore pressures, lower effective stress obliquity and stiffer stress-strain response (at $\tau_c/\sigma'_{vc}=0.2$: $s_{uDSS}/\sigma'_{vc}=0.29$, $\Delta u_s/\sigma'_{vc}=0.07$, $\alpha'_p=17^0$, and $\gamma_p=0.7\%$) than standard tests performed at $\tau_c/\sigma'_{vc}=0$. In contrast, the consolidation shear stress has little effect on the undrained strength for $\tau_c/\sigma'_{vc}<0$, but affects significantly the stress-strain response and the development of shear induced pore pressures.
2. The MIT-E3 model is in very good agreement with the measuremens of pre-peak stress-strain behaviour and effective stress paths in these tests. However, the model tends to overpredict the undrained shear strength for $\tau_c/\sigma'_{vc}>0$ and does not describe accurately the post-peak strain softening measured in these tests.

Overall, the results in figure 14 show important aspects of soil behaviour which can be related directly to the effects of residual axial loads on pile shaft performance.

The ρ-method of estimating capacity (Azzouz et al., 1990) assumes that there is full dissipation of installation excess pore pressures prior to pile loading. However, for large diameter offshore piles, loading is often carried out under conditions of incomplete set-up. These situations can also be readily analyzed using the proposed framework. Figure 15 illustrates predictions of the normalized shaft capacity β/β_∞ (where $\beta_\infty=K_c\rho$) and pore pressure ratio, U, as functions of the dimensionless time factor, T. The results show that the shaft capacity increases by a factor of 2-3 during the set-up process, with most of the strength gain occuring over the time frame, $0.01 \leq T \leq 1.0$.

6.2 Evaluation of Shaft Capacity

The predictions of the undrained strength ratio, ρ, can be evaluated by dividing the measured values of β from rapid axial load tests (which ensure undrained shearing of the clay) and the lateral effective stress ratio measured at the end of set-up, K_c. Measurements of β can be obtained with a high degree of reliability from measurements of the distribution of axial load along the axis of the pile. In contrast, concurrent measurements of the local pore pressures, shear and normal lateral stresses are required in order to interpret the effective stress paths of soil elements at the pile shaft. Reliable data of this type have only

recently been reported from high quality instrumented pile tests in a soft clay (Lehane & Jardine, 1992).

Figure 16a compares the MIT-E3 predictions and measurements of ρ from axial load tests obtained using the PLS cell and instrumented model piles. The PLS data in BBC and Empire clay (R=1.92cm, t_f=10-40secs) (Morrison, 1984; Azzouz & Lutz, 1986) are obtained from axial load cell measurements and provide the average shaft resistance acting between the pile tip and the elevation of the PLS cell. In contrast, six levels of strain gauges are used to estimate the distribution of shaft friction along the length of the Haga piles (L=6m, R=7.6cm, t_f=20mins) (Karlsrud & Haugen, 1985). The results show very good agreement between predictions and measurements of ρ from PLS tests, but underestimate significantly the skin friction ratio reported in the Haga tests. This result can be explained, in large part, by residual loads in the piles which generate significant consolidation shear stresses in the upper half of the pile. Figure 16b compares model predictions of the undrained shear resistance, ρ, as a function of the consolidation shear stress, ρ_c. The results show good agreement with data at depths, z=2 and 3m, but still underpredict the behaviour at z=4m probably due to factors such as the proximity of the pile tip (Whittle, 1991b).

7. Summary and Conclusions

This paper has described the application of a systematic analysis for predicting the performance of driven piles in lightly overconsolidated clays (OCR≤4).The predictions are evaluated through comparisons with field measurements from the Piezo-Lateral Stress (PLS) cell and instrumented model piles. The key components of the analysis are: a) the Strain Path Method, which models the effects of the severe soil disturbances caused by pile installation; and b) MIT-E3, a generalized effective stress soil model with well documented capabilities for describing the non-linear and anisotropic behaviour of K_0-consolidated clays with normalized, rate independent properties. The results focus on conditions during pile installation, stress and pore pressure changes during subsequent consolidation, and the shaft capacity during axial loading:

The Strain Path Method (SPM) provides a realistic model of the mechanics of undrained deep penetration in clays. Predictions using the SPM with the MIT-E3 model give good agreement with the radial effective stresses measured at the pile shaft during steady penetration, but tend to underestimate the installation excess pore pressures. This

latter result probably reflects limitations of the constitutive model for describing the behaviour of structured natural clays.

Radial consolidation around the pile shaft is solved by a coupled, non-linear finite element method with initial conditions from the installation phase and using the MIT-E3 model to describe the effective stress-strain properties of the soil. The consolidation process can be characterized by the pore pressure ratio, $U=\Delta u/\Delta u_i$, the total stress release, H/H_i (where $H=\sigma_r-u_0$), and the set-up effective stress, $K=\sigma'_r/\sigma'_{v0}$, as functions of a dimensionless time factor, T (Fig. 7). The analyses show that the radial distribution of installation excess pore pressures control U, while H/H_i is primarily a function of the non-linear radial compression behaviour of the soil. The paper presents detailed comparisons between predictions and PLS measurements in Boston Blue Clay using average values for the horizontal coefficient of permeability from laboratory tests. The predictions consistently describe the changes in the effective stresses, the total stress release, H/H_i, and the pore pressure ratio, U, throughout consolidation. The predictions are in good agreement with measurements of the radial effective stress at the end of consolidation ($K_c=\sigma'_{rc}/\sigma'_{v0}$) as reported from a number of field sites (Fig. 8). The parameter K_c is affected by the in-situ overconsolidation ratio and sensitivity of the clay.

Predictions of pile shaft performance are presented for rapid axial loading of a long, rigid pile after full dissipation of installation excess pore pressures. The analyses assume that minimum values of the limiting skin friction, f_s, can be estimated from the undrained shear resistance in the soil adjacent to the pile shaft. Results using the MIT-E3 model show that the normalized shear resistance of the soil, ρ ($=f_s/\sigma'_{rc}$, where σ'_{rc} is the radial effective stress at full set-up) is independent of the initial OCR, and can be equated approximately with the undrained strength ratio (s_{uDSS}/σ'_{vc}) of the undisturbed clay measured in an undrained direct simple shear test at OCR≈1.2 (Fig. 13a). The paper discusses other factors affecting the shaft resistance of the pile including partial set-up, drainage conditions in the soil, loading rate and residual loads in the pile. Predictions of the undrained strength ratio, ρ, are in good agreement with field measurements obtained using the PLS cell measured at two sites (Fig. 16).

Acknowledgements

The author would like to thank Prof. M.M. Baligh who initiated and guided the MIT research program on piles in clays. The developments described in this paper were supported by the MIT Sea Grant College program through grant NA86AA-D-SG089 and

by the Henry L. Doherty Professorship in Ocean Engineering. Additional support was provided by a consortium of oil companies including Amoco Production Company, Chevron Oil Field Research, Exxon Production Research, Mobil Research and Development, and Shell Development Company.

References

1. Aubeny, C.P. (1992) "Rational interpretation of in-situ tests in cohesive soils," PhD Thesis, Dept. of Civil Engineering, MIT, Cambridge, MA.
2. Azzouz, A.S. & Lutz, D.G. (1986) "Shaft behaviour of a model pile in plastic Empire clays," ASCE Journal of Geotechnical Engineering, Vol. 112, No. 4, 389-406.
3. Azzouz, A.S. and Morrison, M.J. (1988), "Field Measurements on Model Pile in Two Clay Deposits," ASCE Journal of Geotechnical Engineering, Vol. 114, No. 1, 104-121.
4. Azzouz, A.S., Baligh, M.M. & Whittle, A.J. (1990) "Shaft resistance of friction piles in clay," ASCE Journal of Geotechnical Engineering, Vol. 116, No. 2, 205-221.
5. Baligh, M.M. (1985) "Strain path method," ASCE Journal of Geotechnical Engineering, Vol. 111, No. 9, 1108-1136.
6. Baligh, M.M. (1986a) "Undrained deep penetration: I Shear stresses," Géotechnique, Vol. 36, No. 4, 471-485.
7. Baligh, M.M. (1986b) "Undrained deep penetration: II Pore pressures," Géotechnique, Vol. 36, No. 4, 487-501.
8. Baligh, M.M. & Kavvadas, M. (1980) "Axial static capacity of offshore friction piles in clays," Research Report R80-32, Dept. of Civil Engineering, MIT, Cambridge, MA.
9. Baligh, M.M. & Levadoux, J-N (1980), "Pore pressure dissipation after cone penetration," Research Report R80-11, Dept. of Civil Engineering, MIT, Cambridge, MA.
10. Baligh, M.M., Azzouz, A.S. & Chin, C.T. (1987) "Disturbances due to 'Ideal' tube sampling," ASCE Journal of Geotechnical Engineering, Vol. 113, No. 7, 739-757.
11. Bond, A.J., Jardine, R.J. & Dalton, C.P. (1992) "Design and performance of the Imperial College instrumented pile," ASTM Geotechnical Testing Journal, Vol.14, No. 4, 413-425.
12. Bogard, D., Matlock, H., Audibert, J.M.E. & Bamford, S.R. (1985) "Three years' experience with model pile segment tool tests," Proc. 17th Offshore Tech. Conf., Houston, Paper 4848.

13. Burland, J.B. (1973) "Shaft friction of piles in clay - a simple fundamental approach," Ground Engineering, Vol. 6, No. 3, 30-42.
14. Chandler, R.J. (1968) "The shaft friction of piles in cohesive soils in terms of effective stresses," Civ. Engrg. & Public Works Review, Jan., 48-51.
15. Chin, C.T. (1986) " Open-ended pile penetration in saturated clays," PhD Thesis, Dept. of Civil Enghineering, MIT, Cambridge, MA.
16. Clayton, C.R.I., Khatrush, S.A., Bica, B.V.D., & Siddique, A. (1989) "The use of Hall effect semi-conductors in geotechnical instrumentation," ASTM Geotechnical Testing Journal, Vol. 12, No. 1, 69-76.
17. Coop, M.R. & Wroth, C.P. (1989) "Field studies of an instrumented model pile in clay," Géotechnique, Vol. 39, No. 4, 679-696.
18. DeBorst, R. & Vermeer, P.A. (1984) "Possibilities and limitations of finite element for limit analysis," Géotechnique, Vol. 32, No. 2, 199-210.
19. DeGroot, D.J. (1989) "The Multi-Directional Simple Shear Apparatus with application to the design of offshore Arctic structures," PhD Thesis, Dept. of Civil Engineering, MIT, Cambridge, MA.
20. DeGroot, D.J., Ladd, C.C. & Germaine, J.T. (1992a) "Direct simple shear testing of cohesive soils." Research Report R92-18, Department of Civil Engineering, MIT, Cambridge, MA.
21. Dyvik, R., & Olsen, T.S. (1989) "G_{max} measured in oedometer and DSS tests using bender elements," Proc. 12th Intl. Conf. on Soil Mechs and Found. Engrg., Rio de Janiero, Vol. 1, 39-42.
22. Esrig, M.I., Kirby, R.C., Bea, R.G. & Murphy, B.S. (1977) "Initial development of a general effective stress method for the prediction of axial capacity of driven piles in clay," Proc. 9th Offshore Tech. Conf., Houston, 3, 495-506.
23. Francescon, M. (1983) "Model pile tests in clay - stresses and displacements due to installation and pile loading," PhD Thesis, University of Cambridge.
24. Goto, S., Tatsuoka, F., Shibuya, S., Kim, Y.S., & Sato, T. (1991) "A simple gauge for small strain measurements in the laboratory," Soils and Foundations, Vol. 31, No. 1, 169-180.
25. Jardine, R.J., Symes, M.J., & Burland, J.B. (1984) "The measurement of soil stiffness in the triaxial apparatus," Géotechnique, Vol. 34, No. 3, 323-340.
26. Jardine, R.J., & Christoulas, S. (1991) "Recent developments in defining and measuring static piling parameters," Proceedings, Intl. Conf. on Deep Foundations, Paris, Press Nationale de l'École Nationale des Ponts et Chausées, 713-745.

27. Karlsrud, K. & Haugen, T. (1985) "Axial static capacity of steel model piles in overconsolidated clay," Proc. 11th Intl. Conf. on Soil Mechs and Found. Engrg., San Francisco, 1401-1406.

28. Karlsrud, K. & Nadim, F. (1990) "Axial capacity of offshore piles in clay," Proc. 22nd Offshore Tech. Conf., Houston, Paper 4883.

29. Karlsrud, K., Nadim, F. & Haugen, T. (1986) "Pile in clay under cyclic axial loading, field tests and computational modelling," Proc. 3rd Intl. Conf. on Numerical Methods in Offshore Piling, Nantes, France, 166-190.

30. Karlsrud, K. Borg Hansen, S., Dyvik, R. & Kalsnes, B. (1992) "NGI's pile tests at Tilbrook and Pentre - Review of testing procedures and results," Proc. ICE Conf. on Recent Large Scale Fully Instrumented Pile Tests in Clay, London, July.

31. Karlsrud, K., Kalsnes, B. & Nowacki, F. (1992) "Response of piles in soft clay and silt deposits to static and cyclic loading based on recent instrumented pile load tests," Proc. SUT Conf. on Offshore Site Investigation and Foundation Behaviour, London, September.

32. Kavvadas, M. (1982), "Non-linear consolidation around driven piles in clays," ScD Thesis, Department of Civil Engineering, MIT, Cambridge, MA.

33. Kiousis, P.D., Voyiadis, G.Z. & Tumay, M.T. (1988) "A large strain theory and its application in the analysis of the cone penetration mechanism," Intl. J. for Num. & Anal. Meth. in Geomechanics, Vol. 12, No. 1, 45-60.

34. Kraft, L.M. (1982) "Effective stress capacity model for piles in clay," ASCE Journal of Geotechnical Engineering, Vol. 108, No. 11, 1387-1404.

35. Kraft, L.M., Focht, J.A. & Amerasinghe, S.F. (1981) "Friction capacity of piles driven into clay," ASCE Journal of Geotechnical Engineering, Vol. 107, No. 11, 1521-1541.

36. Lacasse, S. (1979) "Effect of load duration on undrained behaviour of clay and sand," NGI Internal Report 40007-1.

37. Ladd, C.C.& Edgers, L. (1972), "Consolidated-undrained Direct-Simple Shear tests on saturated clays," Research Report R72-82, Dept. of Civil Engineering, MIT, Cambridge, MA.

38. Ladd, C.C. & Foott, R. (1974) "New design procedure for stability of soft clays." ASCE Journal of Geotechnical Engineering, Vol. 100, No. 7, 763-786.

39. Lehane, B. & Jardine, R. (1992) "The behaviour of a displacement pile in Bothkennar clay," Proc. Wroth Memorial Symposium, Oxford.

40. Lemos, L.J. (1985) "The effects of rate on the residual strength of soil," PhD Thesis, Imperial College, London University.

41. Levadoux, J-N. & Baligh, M.M. (1980), "Pore pressures in clays due to cone penetration," Research Report R80-15, Dept. of Civil Engineering, MIT, Cambridge, MA.

42. Malek, A.M., Azzouz, A.S., Baligh, M.M. & Germaine, J.T. (1989) "Behaviour of foundation clays supporting compliant offshore structures," ASCE Journal of Geotechnical Engineering, Vol. 115, No. 5, 615-636.

43. May, R.E. (1987) "A study of the piezocone penetrometer in normally consolidated clay," PhD Thesis, Dept. of Engineering Science, University of Oxford.

44. Morrison, M.J. (1984) " In situ measurements on a model pile in clay," PhD Thesis, Dept. of Civil Engineering, MIT, Cambridge, MA.

45. Nyirenda, Z.M. (1989) "The piezocone in lightly overconsolidated clay," PhD Thesis, Dept. of Engineering Science, University of Oxford.

46. O'Neill, D.A. (1985) "Undrained strength anisotropy of an overconsolidated thixotropic clay," SM Thesis, MIT, Cambridge, MA.

47. Randolph, M.F., Carter, J.P. & Wroth, C.P. (1979), "Driven piles in clay: Effects of installation and subsequent consolidation," Géotechnique, Vol. 29, No. 4, 361-393.

48. Randolph, M.F. & Wroth, C.P. (1981) "Application of the failure state in undrained simple shear to the shaft capacity of driven piles," Géotechnique, Vol. 31, No. 1, 143-157.

49. Roscoe, K.H. & Burland, J.B. (1968), "On the Generalized Behaviour of Wet Clays," Engineering Plasticity, Eds. J. Heymann & F.A. Leckie, Cambridge University Press, 535-609.

50. Roy, M., Blanchet, R., Tavenas, F. & LaRochelle, P. (1981) "Behaviour of a sensitive clay during pile driving," Canadian Geotechnical Journal, Vol. 18, No. 1, 67-85.

51. Teh, C-I & Houlsby, G.T. (1991) "An analytical study of the cone penetration test in clay," Géotechnique, Vol. 41, No. 1, 17-35.

52. Ting, N-H., Onoue, A., Germaine, J.T., Whitman, R.V. & Ladd, C.C. (1990) "Effects of disturbance on soil consolidation with vertical drains," Research Report R90-11, Dept. of Civil Engineering, MIT, Cambridge, MA.

53. Whittle, A.J. (1987) "A constitutive model for overconsolidated clays with application to the cyclic loading of friction piles," ScD Thesis, Dept. of Civil Engineering, MIT, Cambridge, MA.

54. Whittle, A.J. (1990) "A constitutive model for overconsolidated clays," MIT Sea Grant Report, MITSG90-15.

55. Whittle, A.J. (1991a) "Evaluation of a constitutive model for overconsolidated clays," Accepted for publication, Géotechnique.

56. Whittle, A.J. (1991b) "Interpretation of pile load tests at the Haga site," Proc. ASME Conf. on Offshore Mechs. & Arctic Engrg. (OMAE'91), Stavangar, Vol. 4, 267-275.

57. Whittle, A.J., Baligh, M.M., Azzouz,A.S. & Malek, A.M. (1988) "A Model for Predicting the Performance of TLP Piles in Clay," Proc. 5th Intl. Conf. on Behaviour of Offshore Structures (BOSS'88), Trondheim, Vol. 1, 97-112.

58. Whittle, A.J. & Baligh, M.M. (1988) "The behaviour of piles supporting tension leg platforms, Results of Phase III," Report submitted to Joint Oil Industry, Dept. of Civil Engineering, MIT, Cambridge. MA.

59. Whittle, A.J., Aubeny, C.P., Rafalovich, A., Ladd, C.C. & Baligh, M.M. (1991) "Interpretation of in-situ tests in cohesive soils using rational methods," Research Report R91-01, Dept. of Civil Engineering, MIT, Cambridge, MA.

60. Whittle, A.J., DeGroot, D.J., Ladd, C.C. & Seah, T.H. (1992) "Model prediction of the anisotropic properties of Boston Blue Clay," *submitted to ASCE Journal of Geotechnical Engineering*.

61. Wood, D.M. (1981) "True triaxial tests on Boston Blue Clay,". Proceedings 10th Intl. Conf. on Soil Mechs. and Foundation Engrg., Stockholm, 825-830.

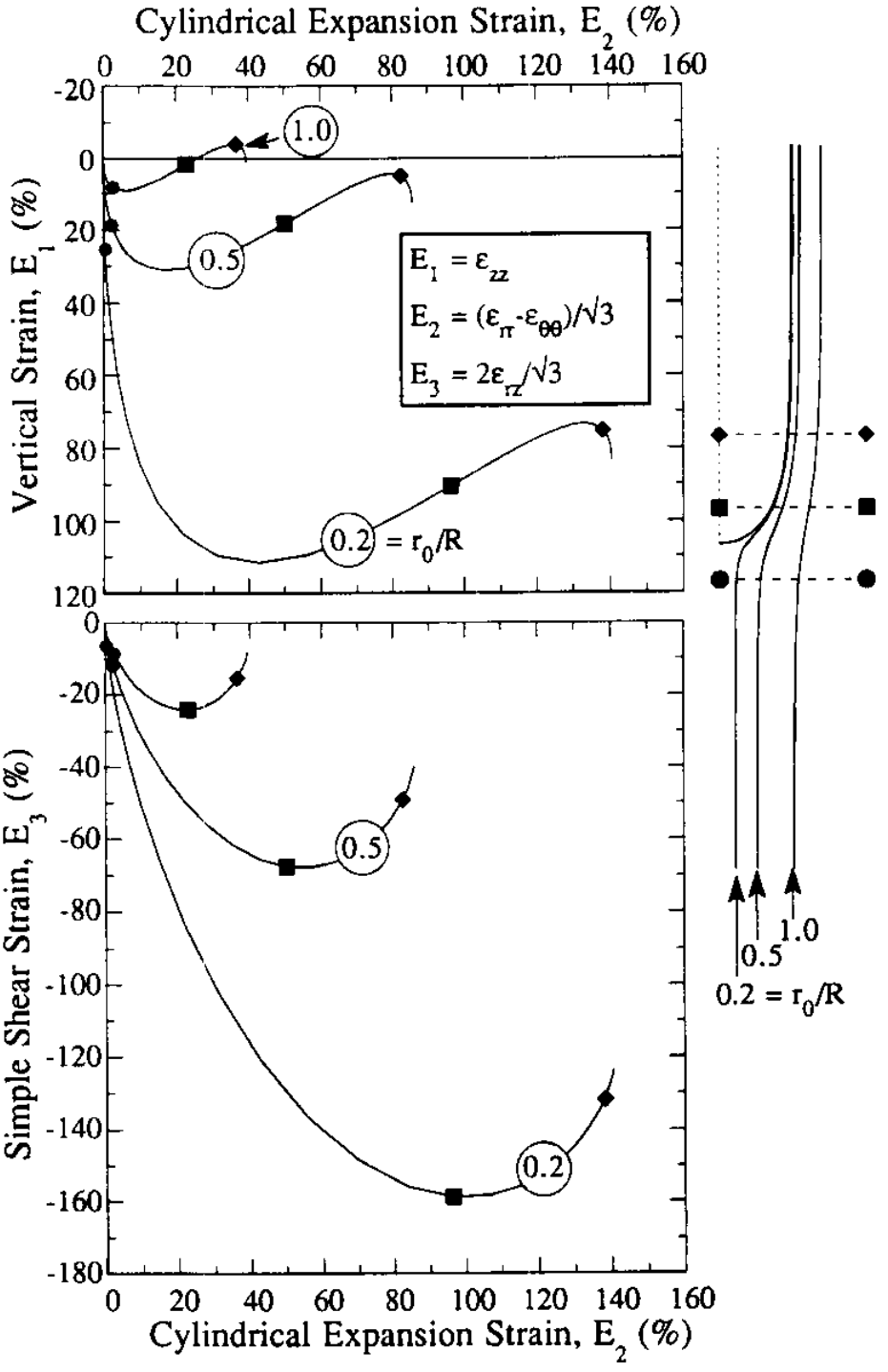

Fig. 1a Strain Paths during Simple Pile Penetration
(after Baligh, 1985)

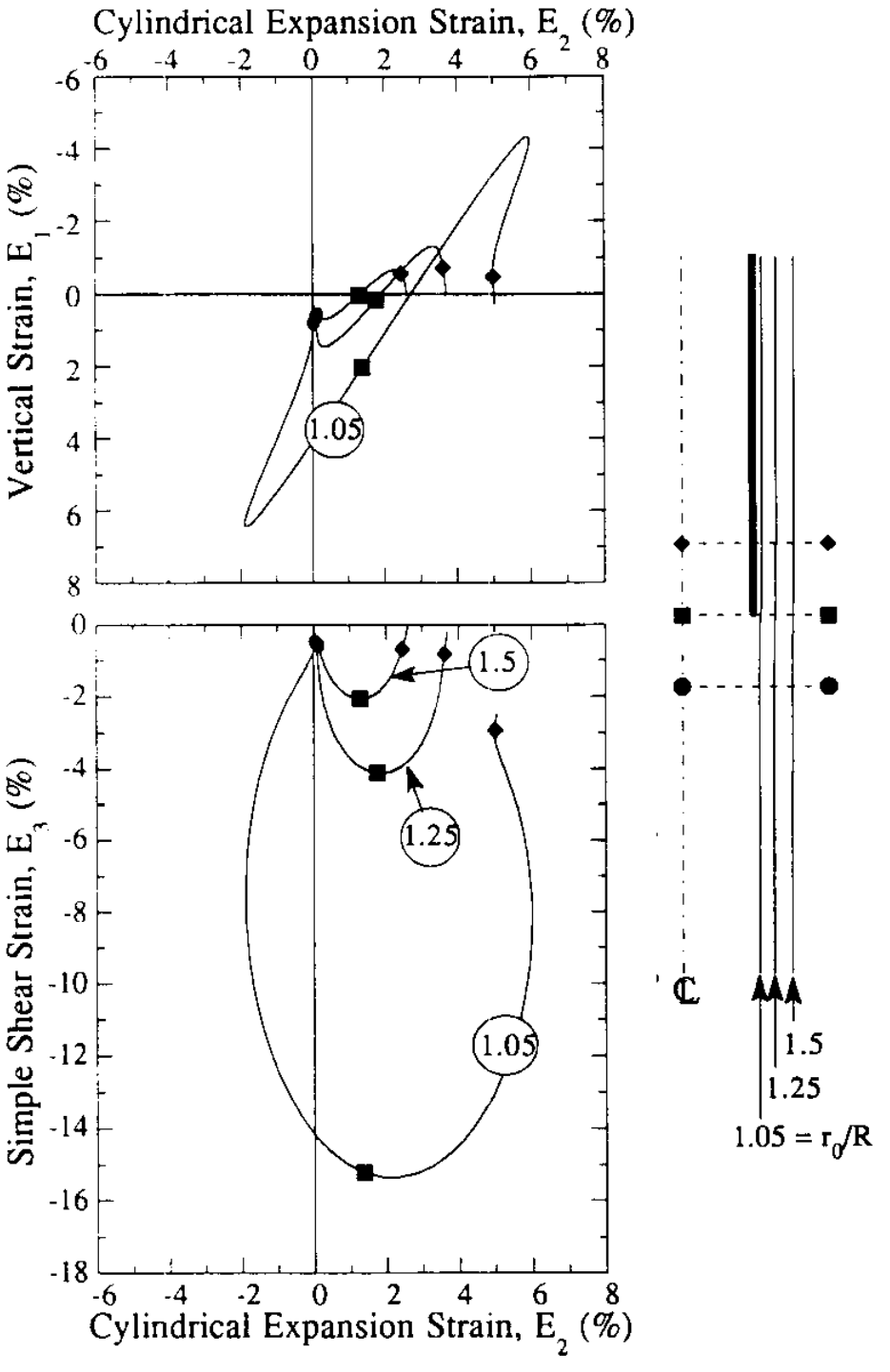

Fig. 1b Strain Paths during Unplugged Penetration of Open-Ended Pile, B/t=40 (after Chin, 1986)

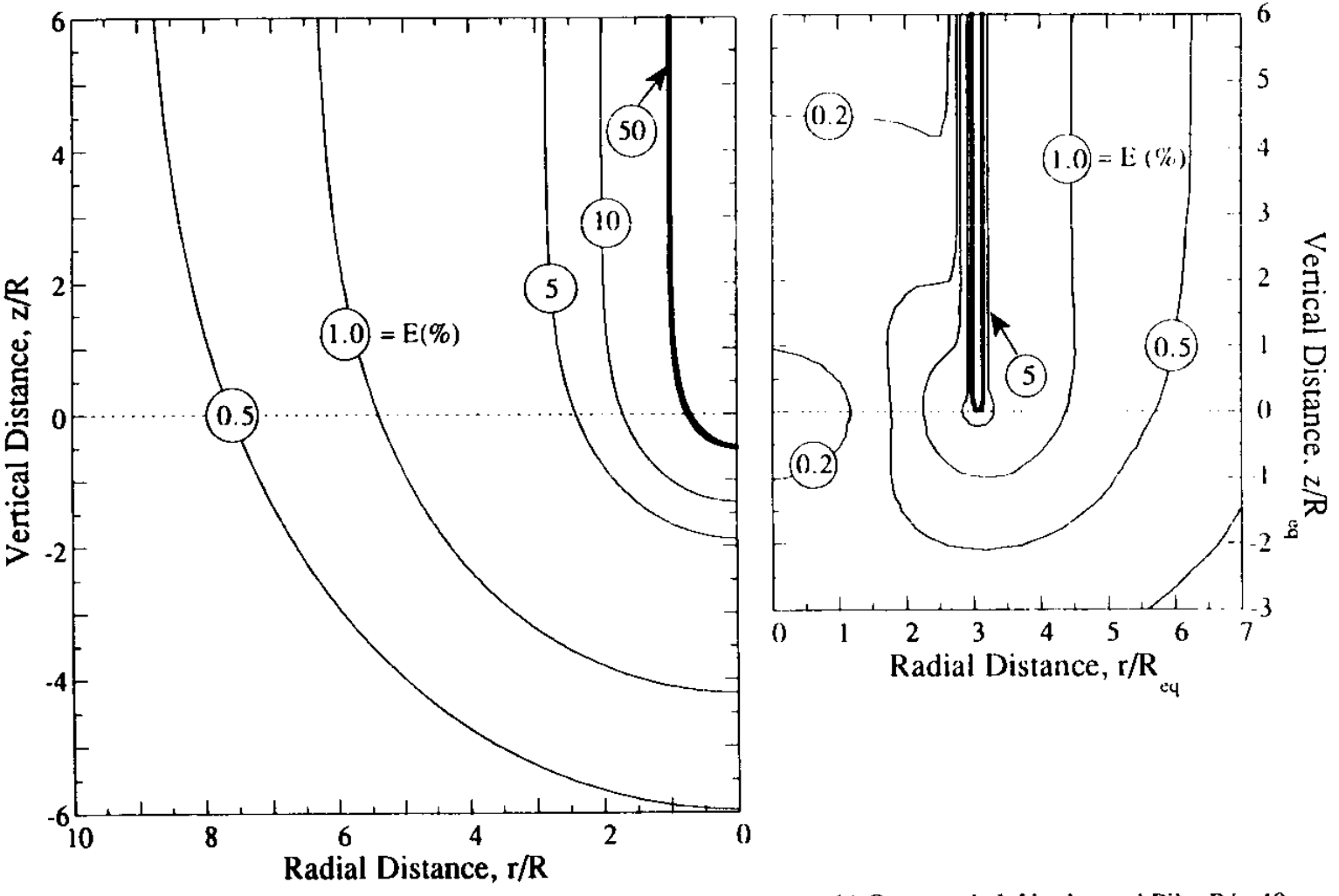

a) Simple Closed-Ended Pile, b) Open-ended, Unplugged Pile, B/t=40

Fig. 2 Shear Strains during Pile Installation

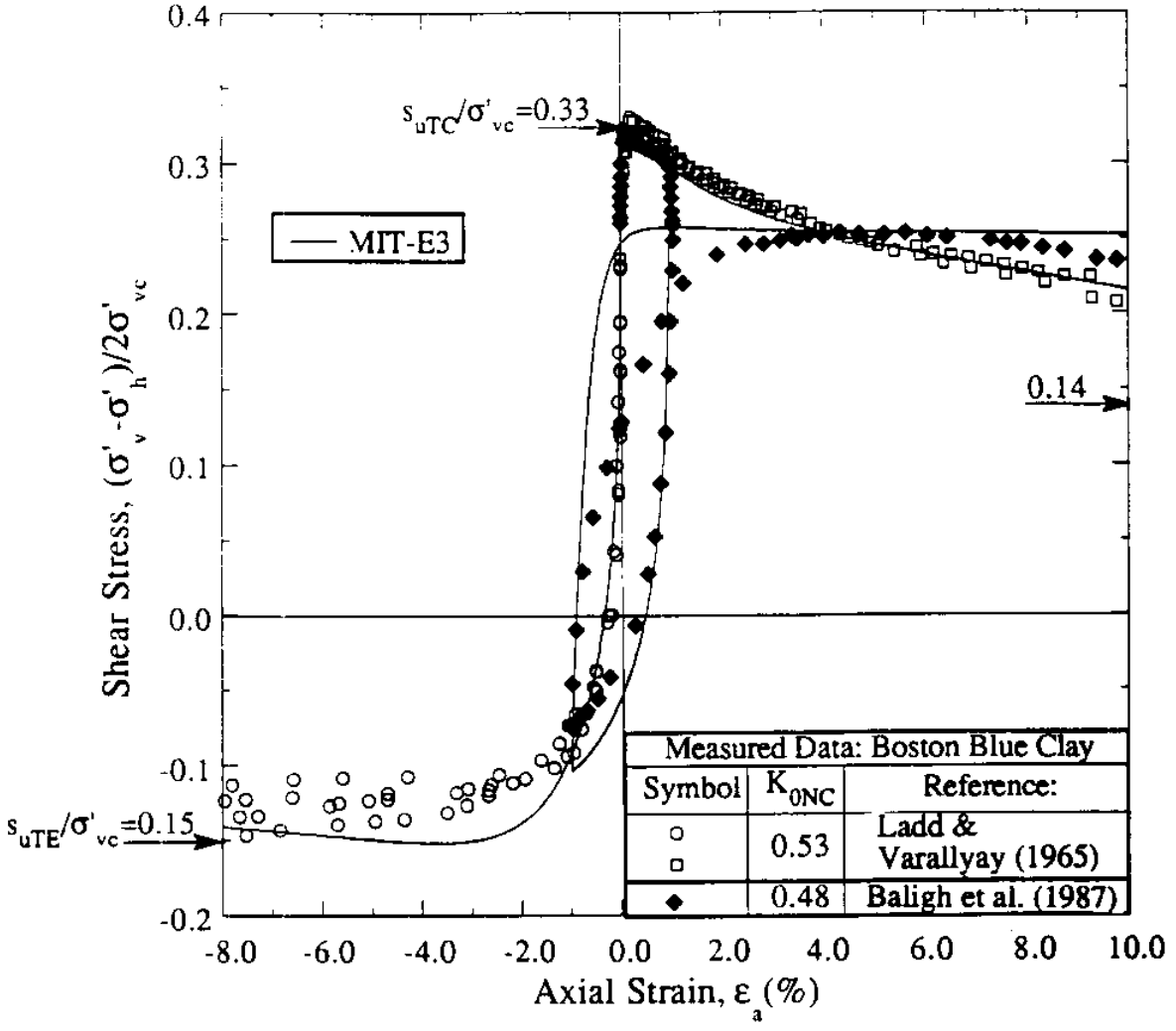

Figure 3a. Comparison of MIT-E3 Predictions and Measured Data for Undrained Triaxial Shearing of K_0-Normally Consolidated Boston Blue Clay

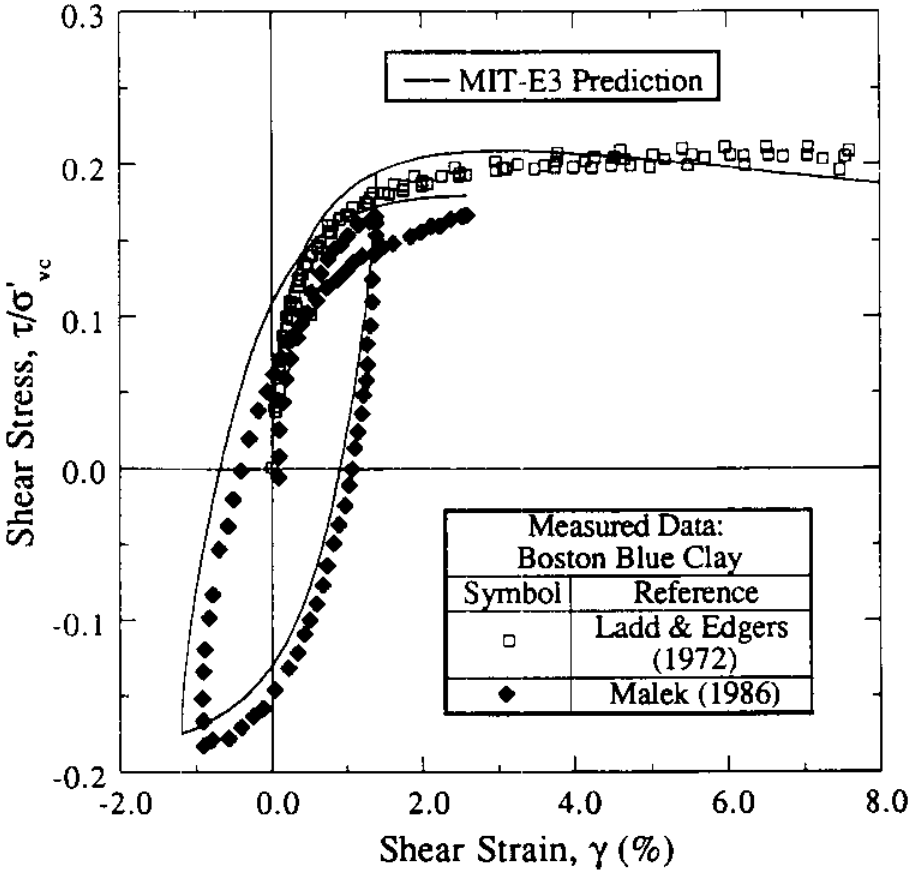

Figure 3b. Comparison of Model Predictions and Measured Data for Direct Simple Shear of K_0-Normally Consolidated Boston Blue Clay

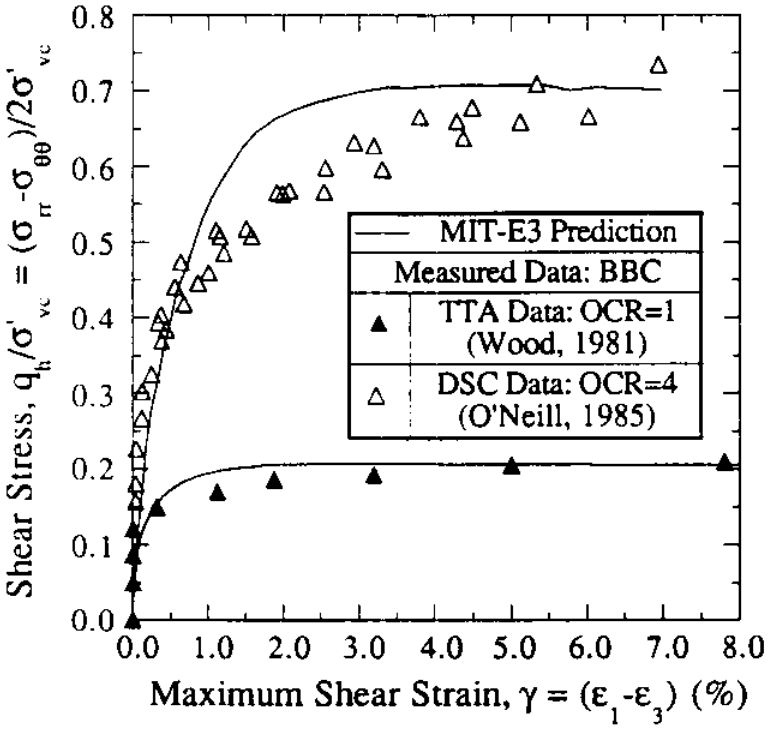

Figure 3c. Comparison of Model Predictions and Measured Data for a Pressuremeter Mode of Shearing of K_0-Consolidated BBC

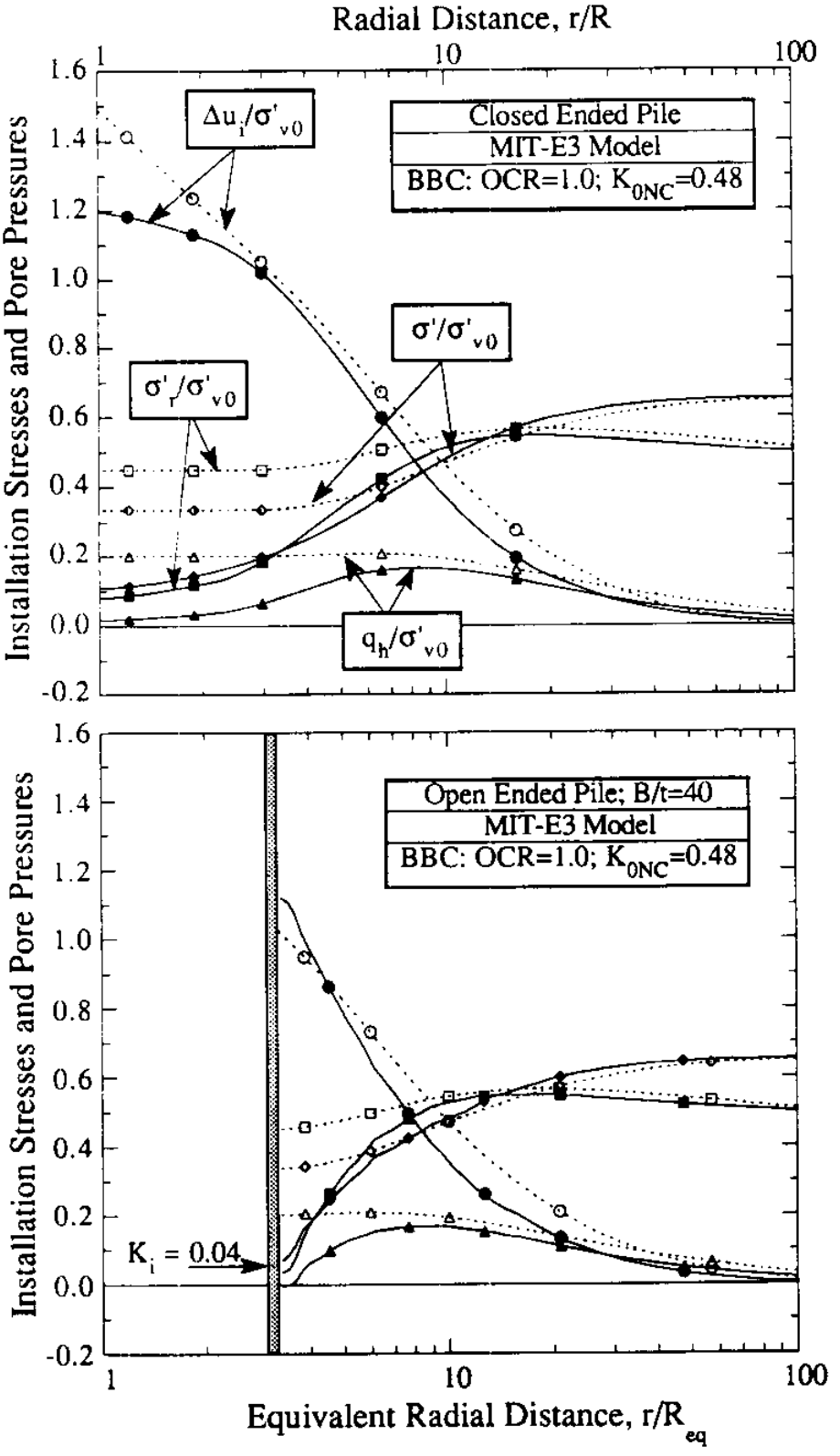

Stress Component:	$\Delta u_i/\sigma'_{v0}$	σ'_r/σ'_{v0}	σ'/σ'_{v0}	q_h/σ'_{v0}
Strain Path Method	—●—	—■—	—◆—	—▲—
Cavity Expansion Method	···○···	···□···	···◇···	···△···

Fig. 4 Strain Path Predictions of Installation Stresses in K_0-Normally Consolidated BBC

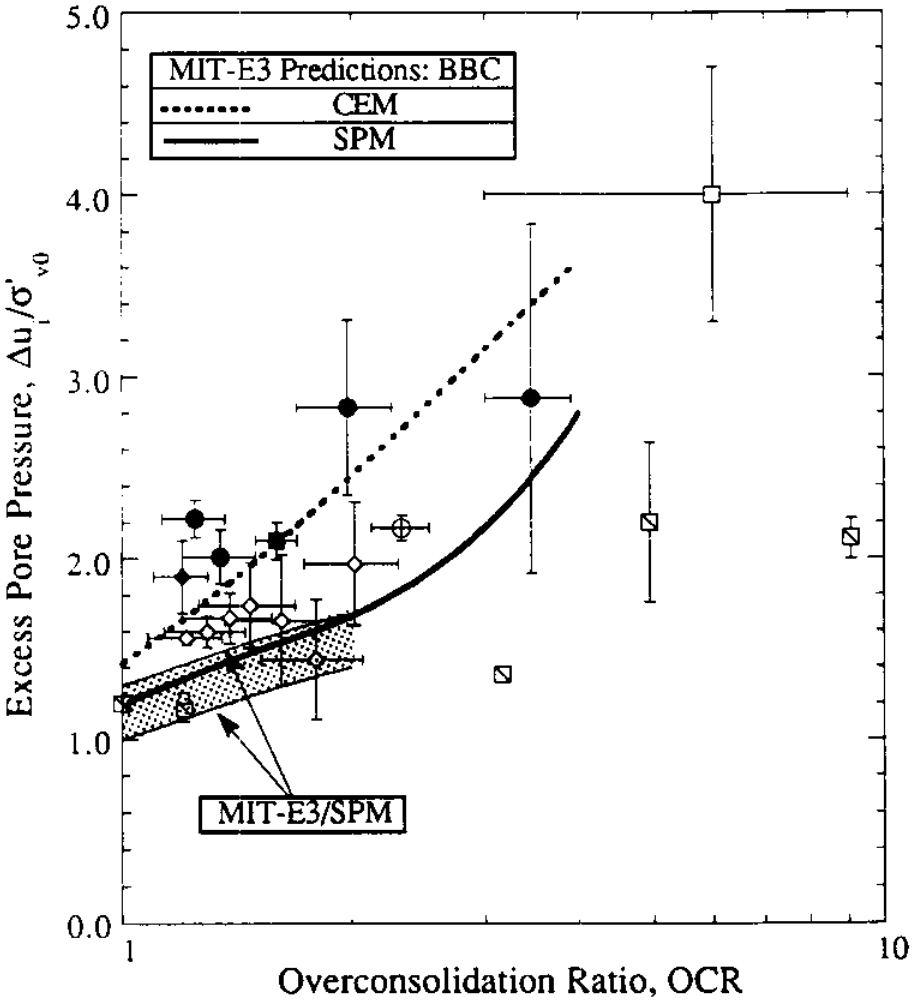

Measured Data		
Symbol	Clay	Reference
●	BBC	Morrison (1984)
○	St Alban	Roy et al. (1981)
◆	Onsøy	Karlsrud et al. (1992)
■	Empire	Azzouz & Lutz (1987
□	Haga	Karlsrud & Haugen 91985)
◇	Inchinnan	May (1987)
▨	Kaolin	May (1987), Nyirenda (1989)

Fig. 5 Evaluation of Installation Pore Pressures at Pile Shaft

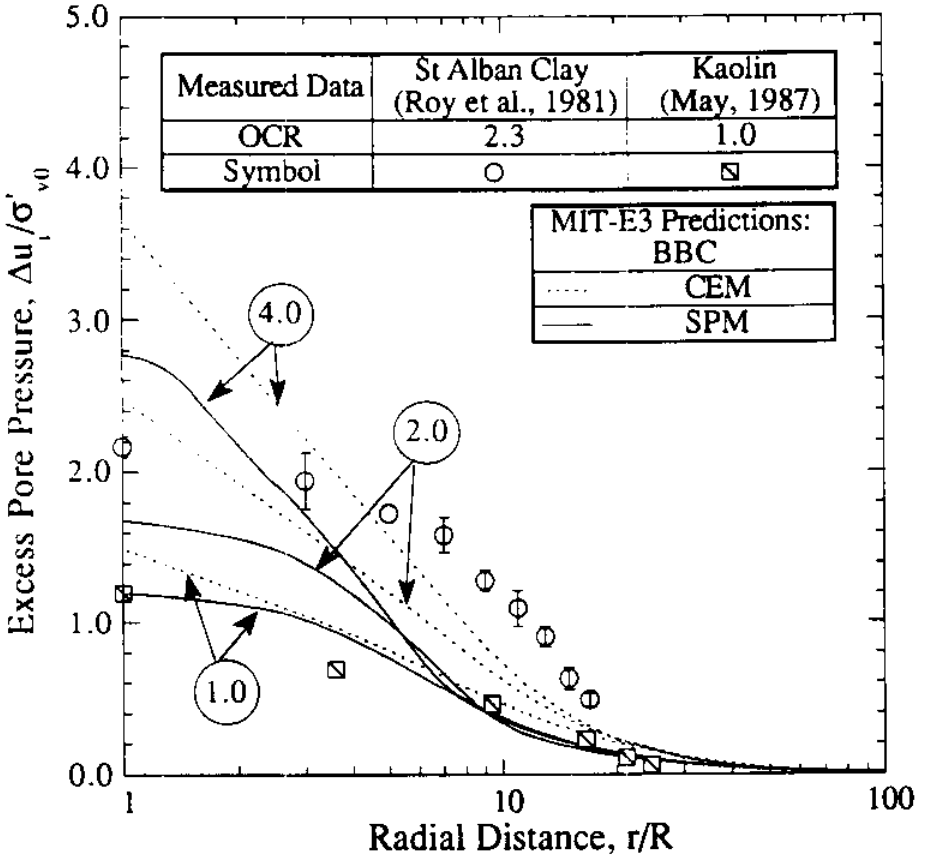

Fig. 6 Distribution of Excess Pore Pressures during Installation

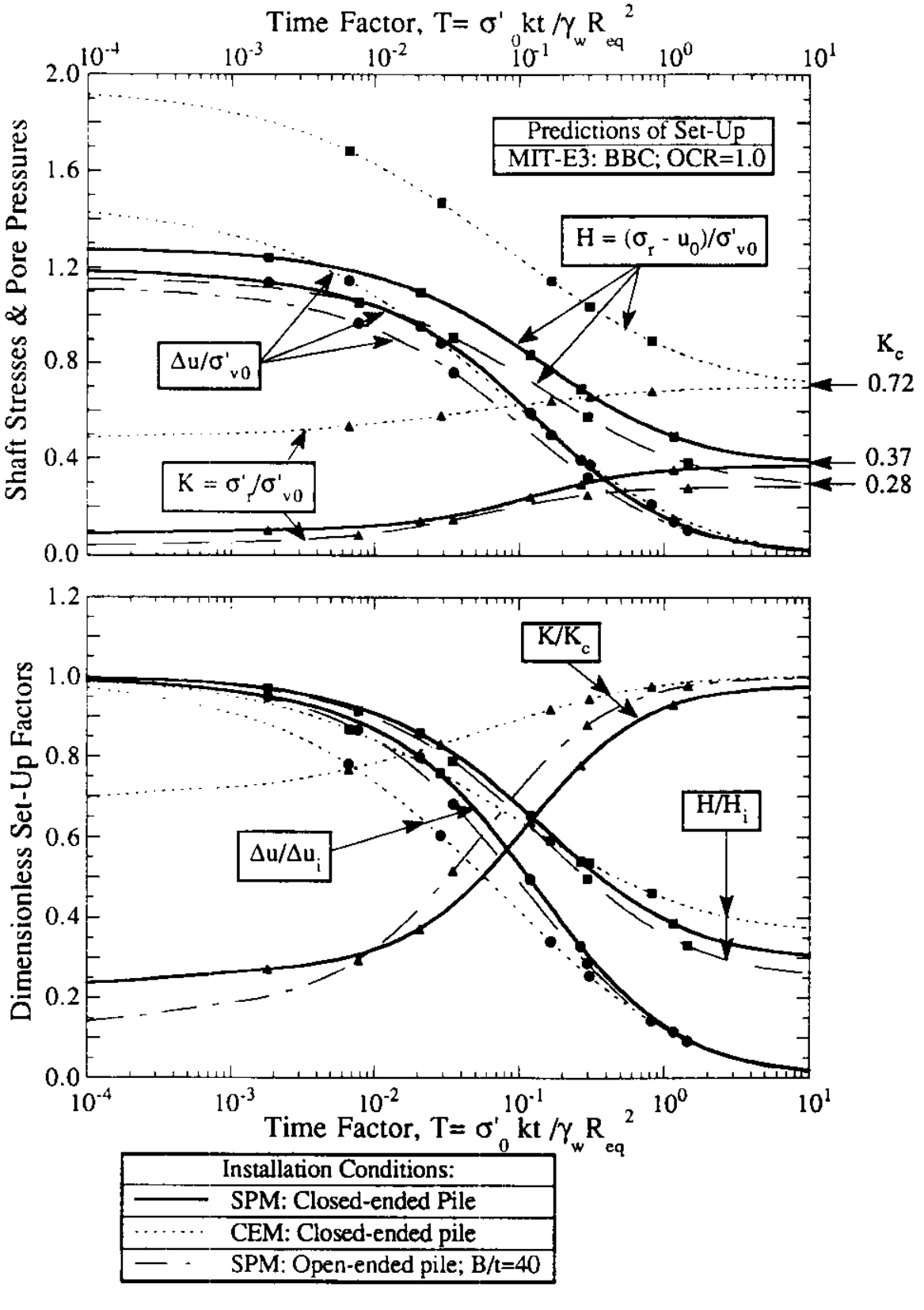

Fig. 7 Typical Predictions of Consolidation at the Pile Shaft in K_0-Normally Consolidated BBC

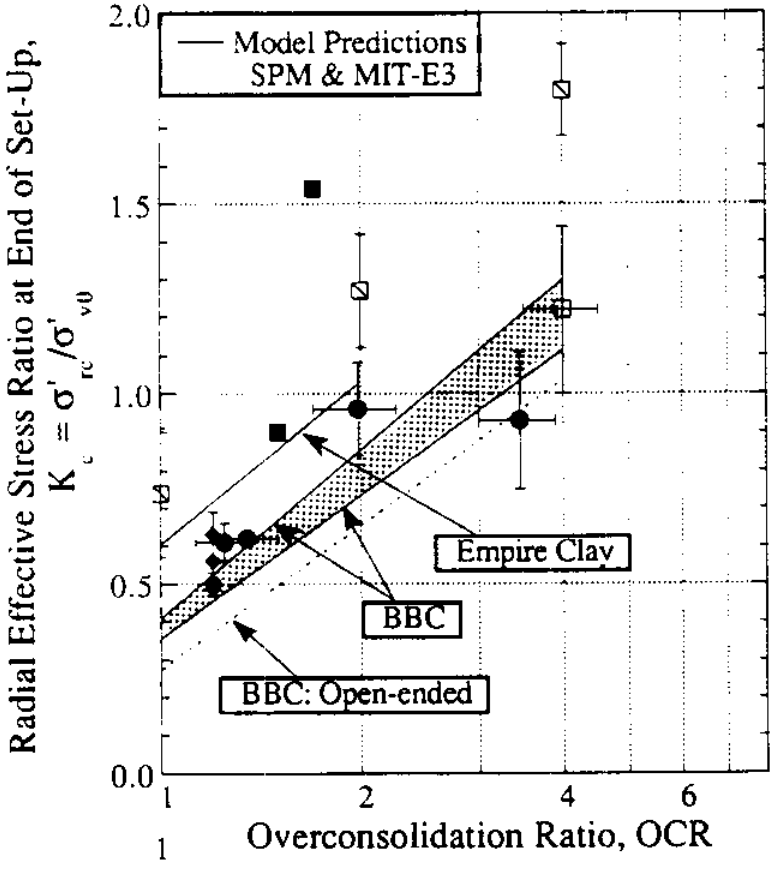

Measured Data		
Symbol	Clay	Reference
●	BBC	Morrison (1984)
◆	Onsøy	Karlsrud et al. (1992)
■	Empire	Azzouz & Lutz (1986)
□	Haga	Karlsrud & Haugen (1985)
⧅	Kaolin	Francescon (1983)

Fig. 8 Evaluation of Radial Stress at End of Set-Up

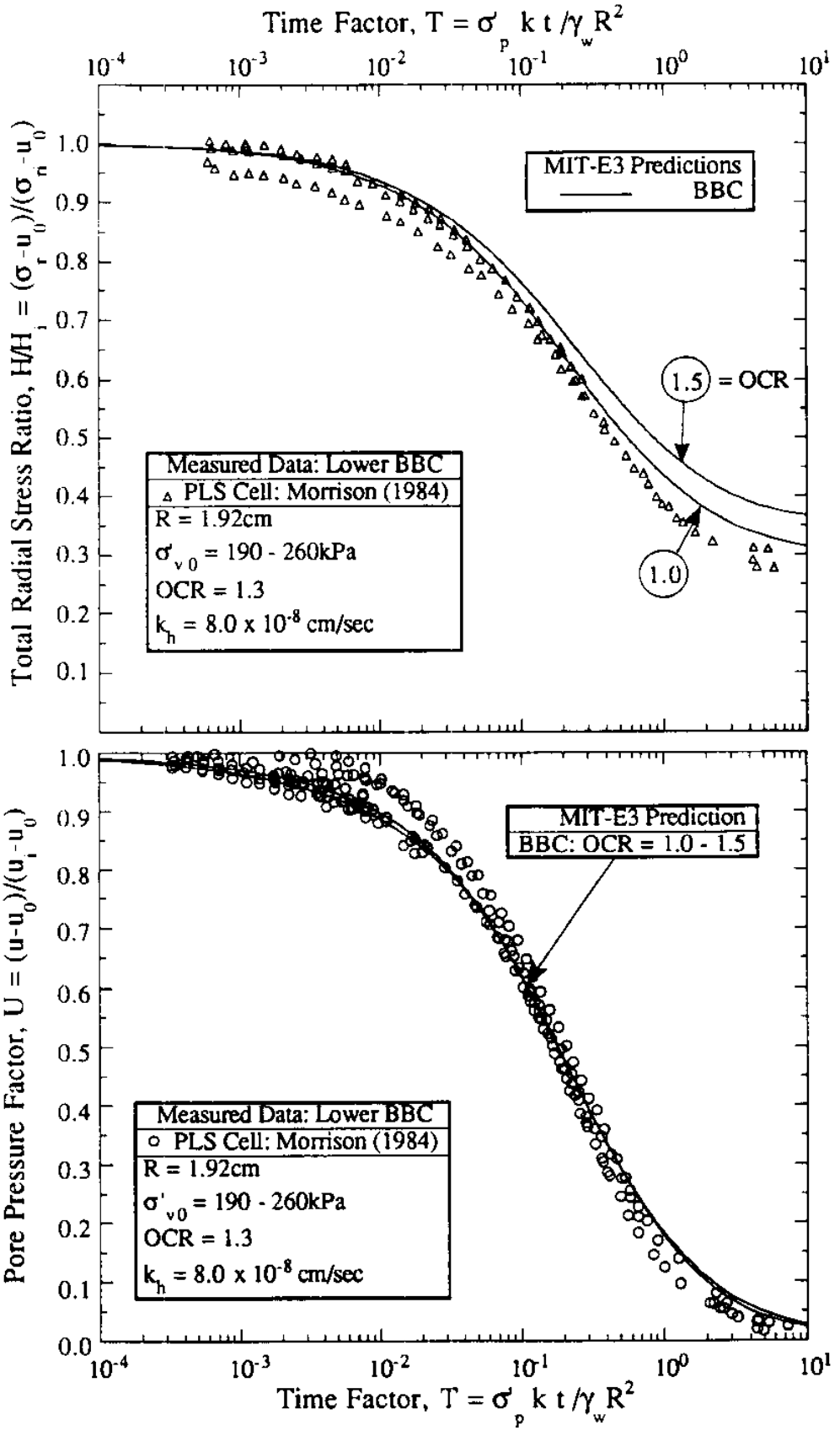

Fig. 9 Comparison of Predictions and Measurements during Consolidation in Boston Blue Clay

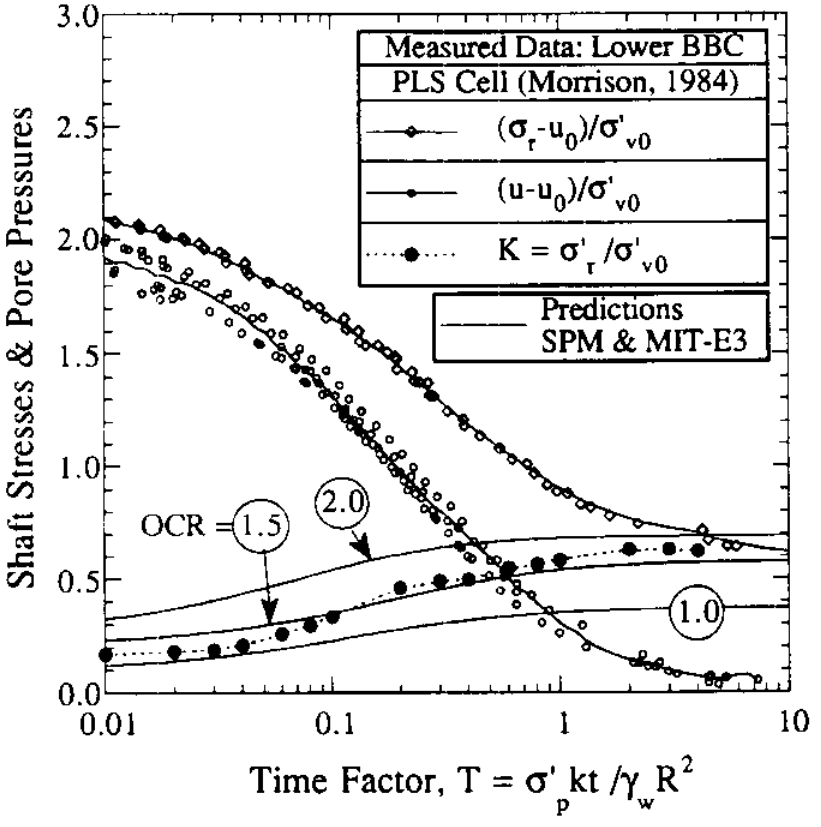

Fig. 10 Evaluation of Effective Stress Set-Up in Lower BBC

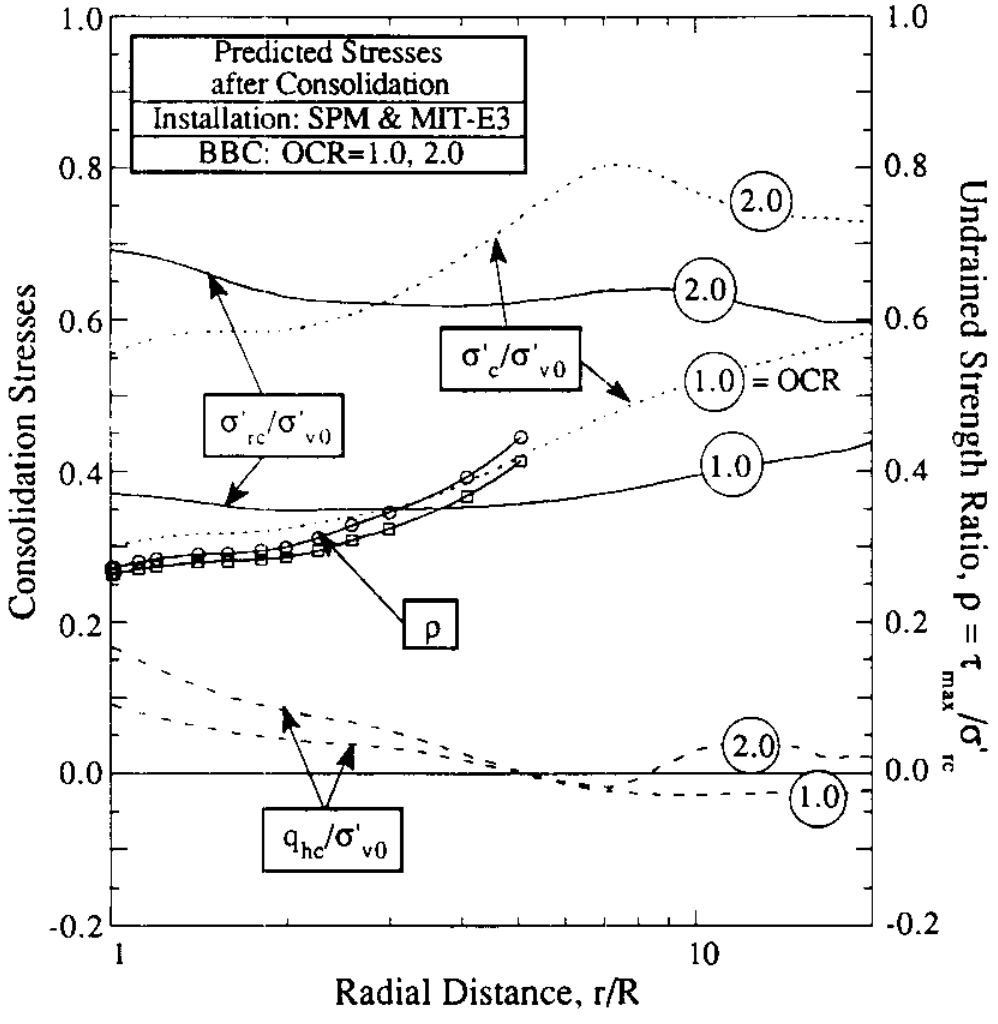

Fig. 11 Predicted Stress Conditions at the End of Consolidation

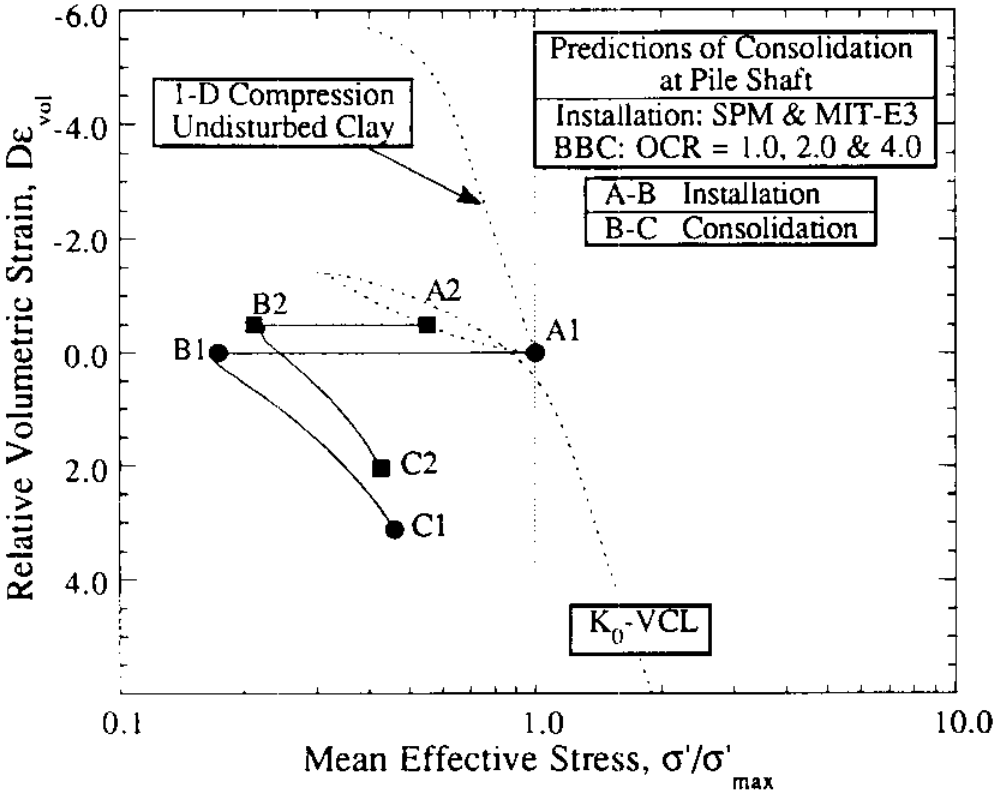

Fig. 12 Predicted Volumetric Behaviour of Soil Elements Adjacent to the Pile Shaft

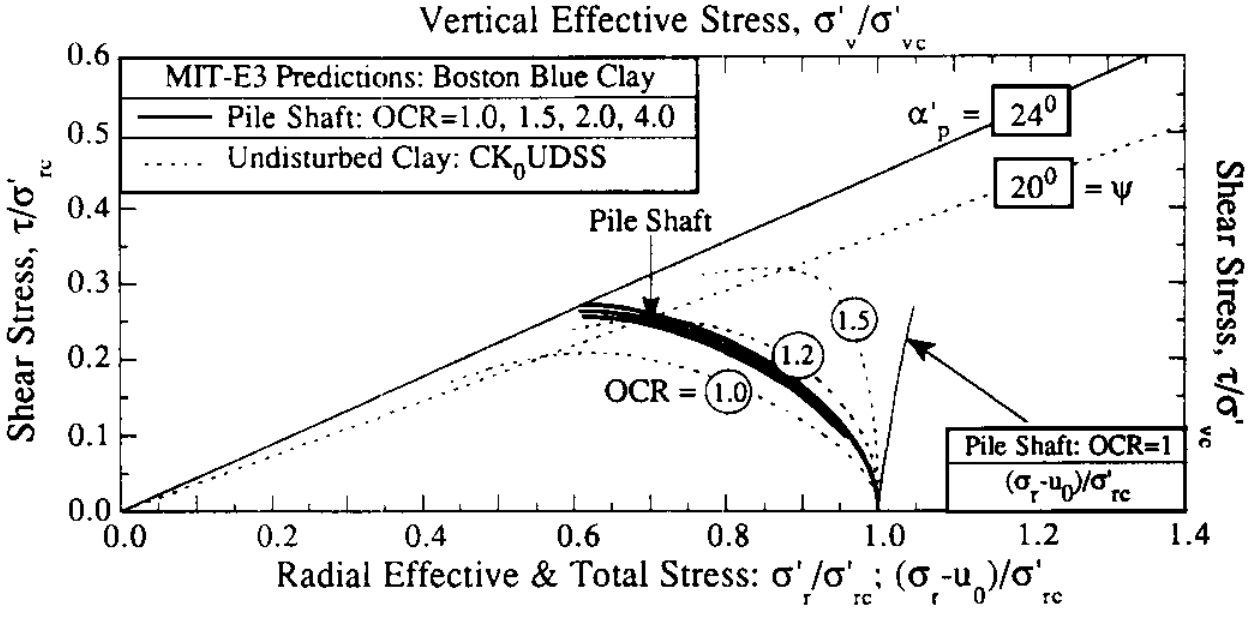

Fig. 13 a) Undrained Shear Behaviour

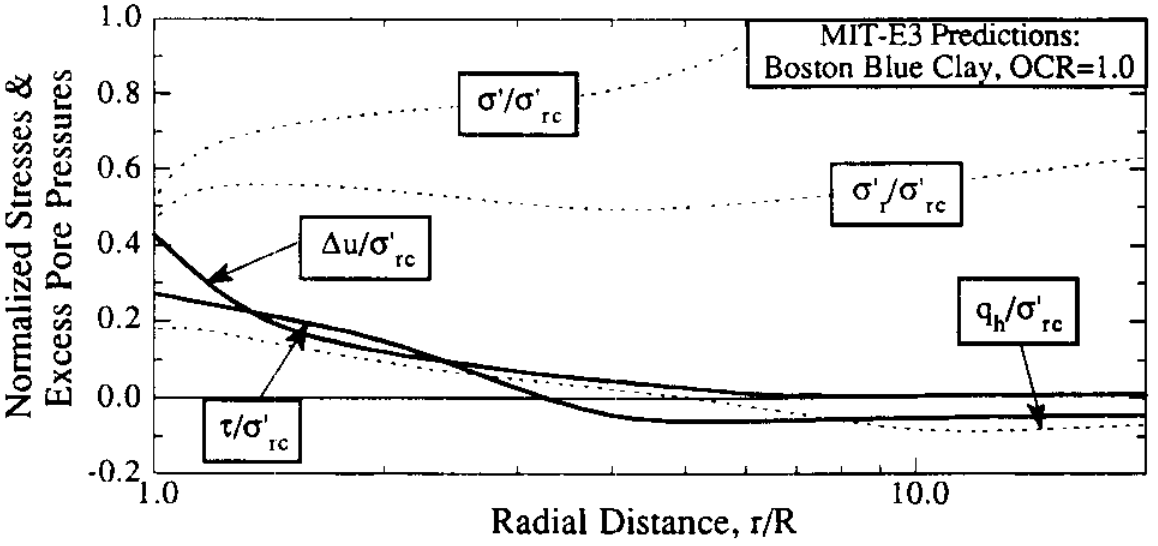

b) Radial Distribution of Stresses and Excess Pore Pressures at Peak Shear Resistance

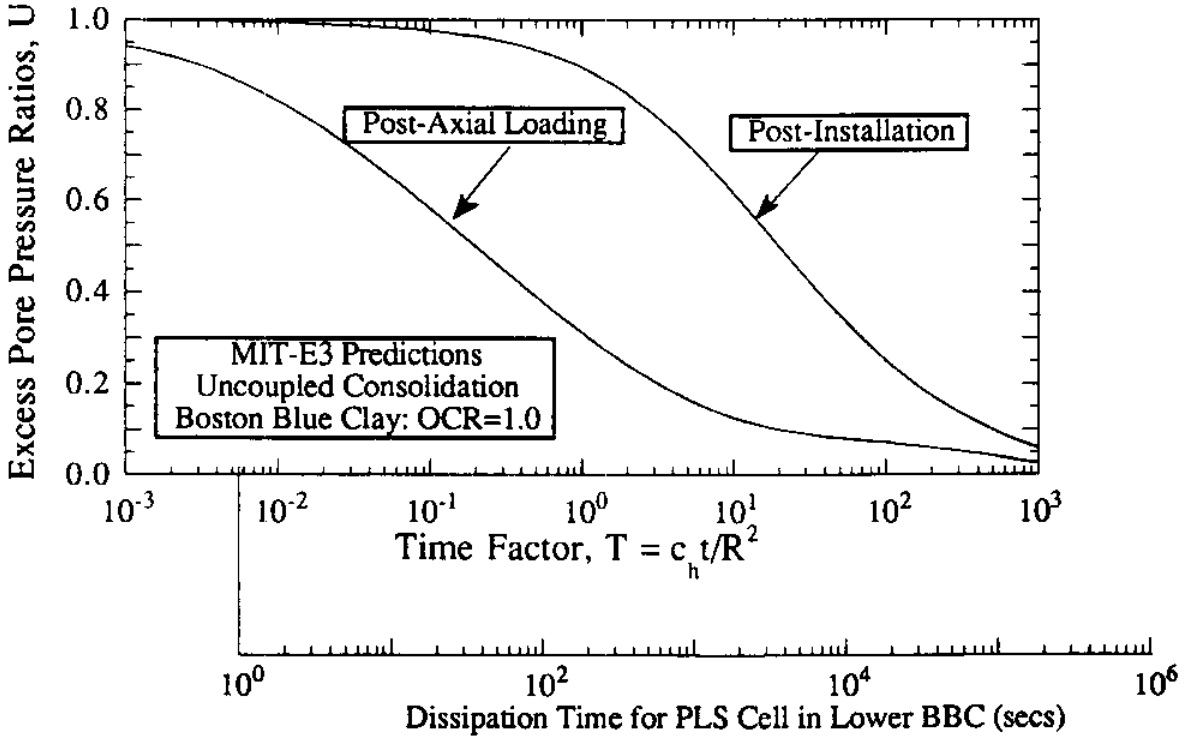

c) Dissipation of Excess Pore Pressures

Fig. 13 MIT-E3 Predictions of Soil Behaviour for Elements at the Pile Shaft during Axial Loading

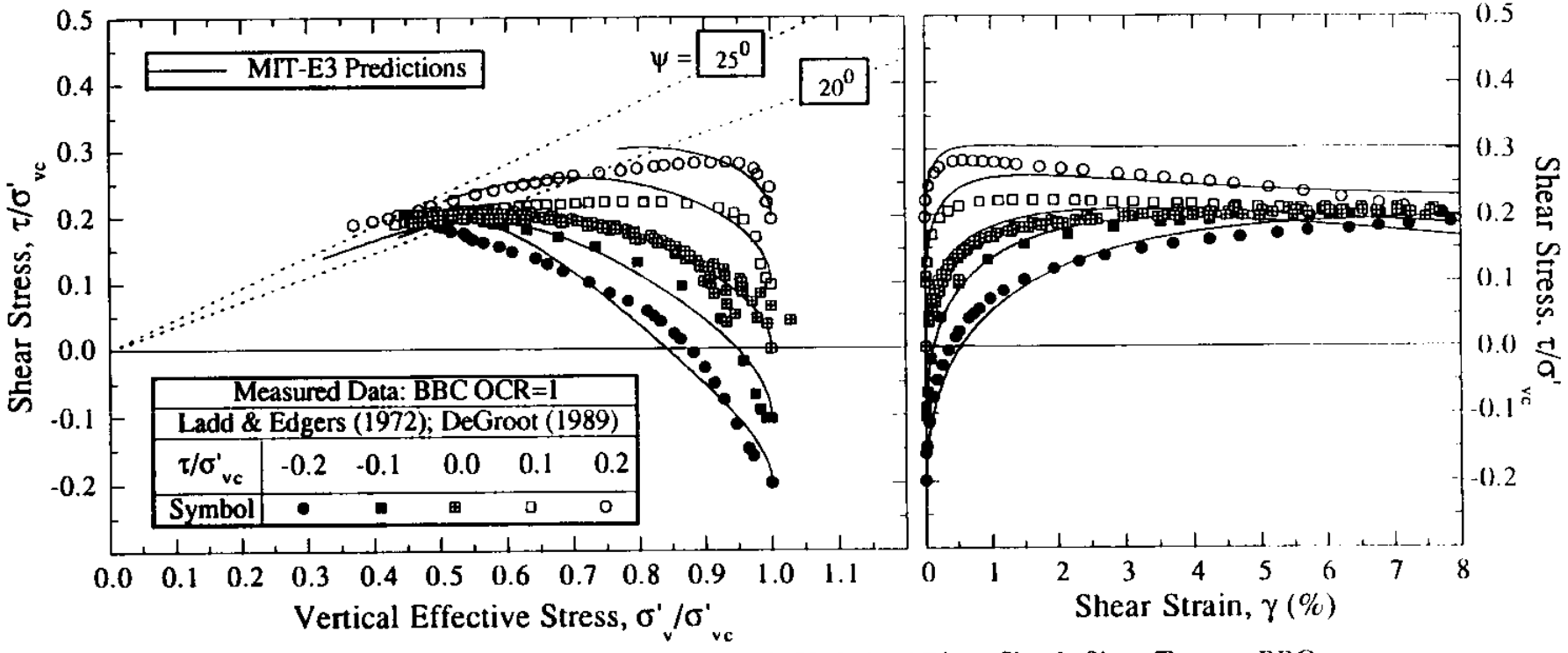

Fig. 14 Effect of Consolidation Shear Stress in Undrained Direct Simple Shear Tests on BBC

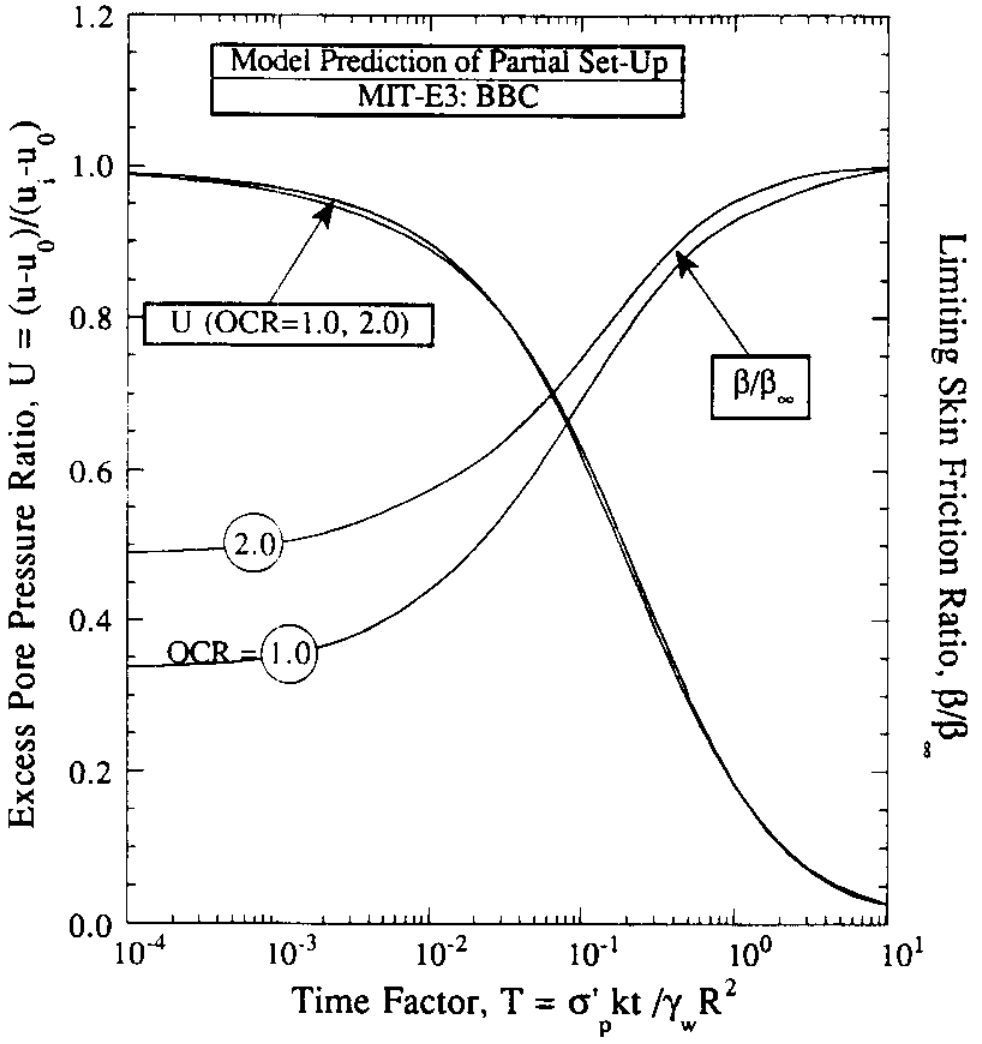

Note: $\beta_\infty = K_c \rho$

Fig. 15 Prediction of Shaft Capacity for Partial Set-Up in BBC

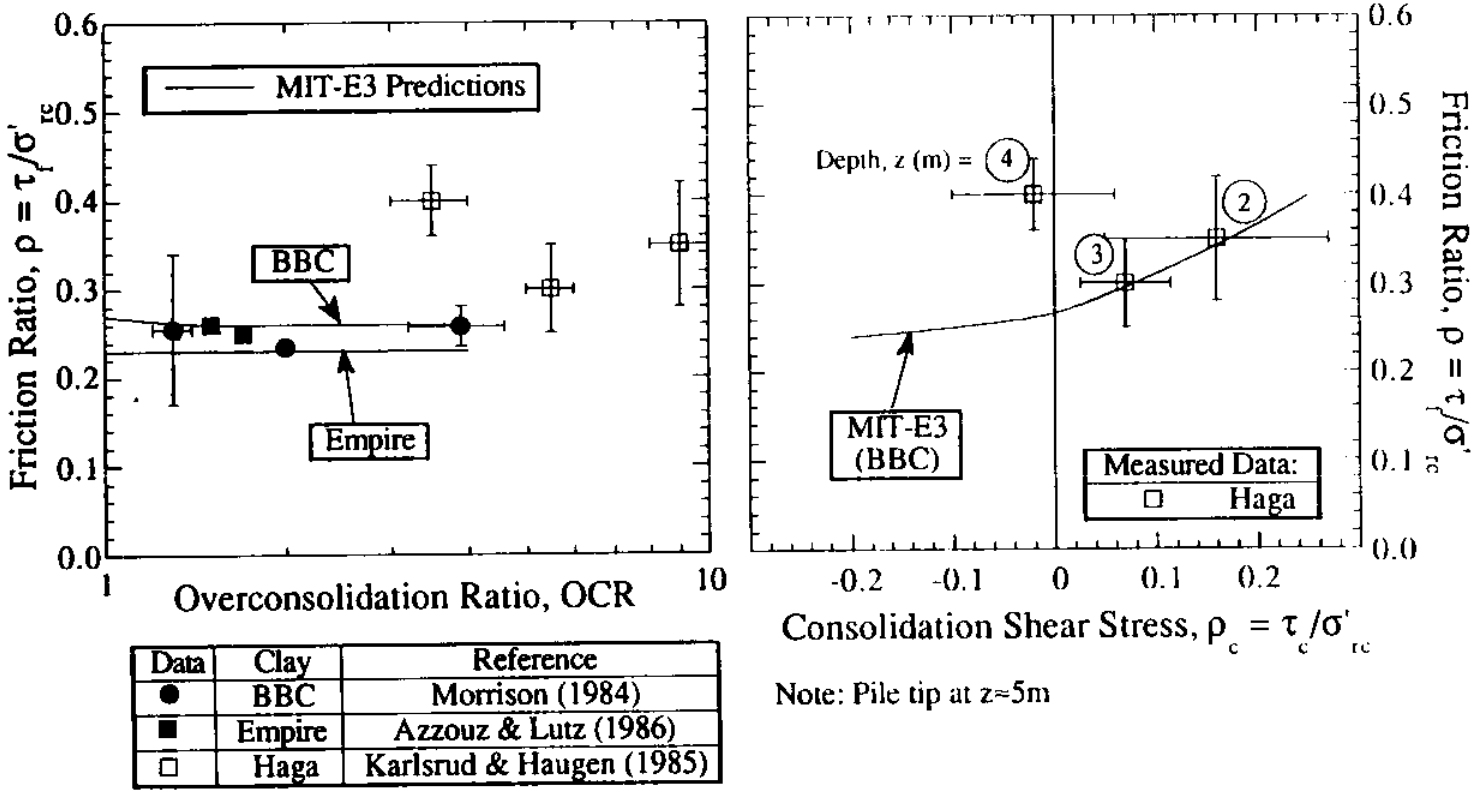

Data	Clay	Reference
●	BBC	Morrison (1984)
■	Empire	Azzouz & Lutz (1986)
□	Haga	Karlsrud & Haugen (1985)

Note: Pile tip at z≈5m

Fig. 16 Evaluation of the Undrained Strength Ratio, ρ, of Soil Adjacent to the Pile Shaft